TOLUENE ALKYLATION WITH PROPYLENE AND ETHYLENE ON ACIDIC MORDENITE ZEOLITE

by

Hanna Monroe

A thesis submitted to the Faculty and The Board of Trustees of the Colorado School of Mines in partial fulfillment of the requirements of the degree of Master of Science (Chemical Engineering).

Golden, Colorado
Date: _____

Signed: _____

Hanna Monroe

Signed: _____

Dr. Stephanie Kwon

Thesis Advisor

Golden, Colorado

Date: _____

Signed: _____

Dr. Anuj Chauhan

Professor and Head

Department of Chemical and Biological Engineering

ABSTRACT

Aromatic alkylation with ethylene and propylene are important reactions to produce cumene and ethylbenzene. Acidic zeolites have been widely used in the petrochemical industry since the 1980s for benzene alkylation due to their high reactivity, non-corrosivity, and environmentally friendly nature compared to traditional liquid acids. There are several challenges in the commercial benzene alkylation processes such as catalyst deactivation via alkene dimerization in addition to energy intensive and costly downstream separation processes primarily due to the high benzene to alkene ratio required to form the desired monoalkylated products. A variety of zeolites have been used for commercial benzene alkylation, however, there is still a lack of literature aimed at understanding how the microporous structures of zeolitic framework and the locations of acidic H^+ sites impact their catalytic selectivity and stability. Furthermore, the reaction pathways of benzene alkylation on solid acids have remained uncertain.

In this work, we combine kinetic, spectroscopic, and theoretical methods to identify the reaction pathways and to understand how the microporous structure impacts the reactivity and stability, taking the toluene-ethylene reaction as a model reaction. We reveal that exchanging H^+ sites in the 8-membered ring (8-MR) significantly improves the stability of acidic mordenite zeolites by lowering the contribution of alkene dimerization reactions that lead to coke formation. By combining kinetic and spectroscopic techniques, we show that protons are saturated with π-bonded toluene, which sequentially react with ethylene to form ethyl toluene.

These results can be utilized to provide design strategies for solid acid catalysts used in benzene alkylation with improved stability, selectivity, and reactivity.

TABLE OF CONTENTS

LIST OF FIGURES

LIST OF TABLES

LIST OF SCHEMES

ACKNOWLEDGEMENTS

First of all, I would like to thank my thesis advisor Dr. Stephanie Kwon for providing me with guidance and support on this journey to my master's degree. Thank you for assisting me in becoming a better researcher and believing in my ability to succeed by giving me a project that provided me with hands on experience in heterogenous catalysis processes.

I would like to acknowledge members of the Kwon lab group: Manasi Vyas, Yingxue Bian, Michelle Nolen, Emily Volk, and Kemakorn Ithisuphalap who provided valuable input and advice in my search to better my scientific endeavors. It was truly a pleasure to get to work with like-minded individuals who also have a passion for research. A special thank you to Michelle Nolen and Kemakorn Ithisuphalap for helping me with this thesis by providing computation and experimental results.

Lastly, I would like to thank my husband, parents, and sister for supporting me through my decision to pursue higher education. I would not be here without your encouragement and advice.

CHAPTER 1

INTRODUCTION

1.1 Benzene Alkylation Overview

Benzene alkylation with light alkenes is a key reaction in the petrochemical industry to produce cumene and ethylbenzene (Fig 1.1). The demand for products like cumene and ethylbenzene increases every year due to their ability to form phenol, styrene, and acetone which are chemical intermediates used to make commodity products like polystyrene, polycarbonate, epoxy resins, and poly(p-methylstyrene).[3–6] Traditional alkylation processes utilized solid acid catalysts such as $AlCl_3$ and solid phosphorous acid; however, due to the corrosivity and toxicity of acidic waste generated from these processes, they have been widely replaced by zeolite catalysts.[7] Since the 1980s, companies such as DOW Chemical, Lummus-UOP, and Mobil-Badger have developed commercially licensed zeolite catalyzed alkylation processes which overcome the drawbacks associated with previous solid acid catalysts by providing more environmentally friendly and efficient processes.[4,7]

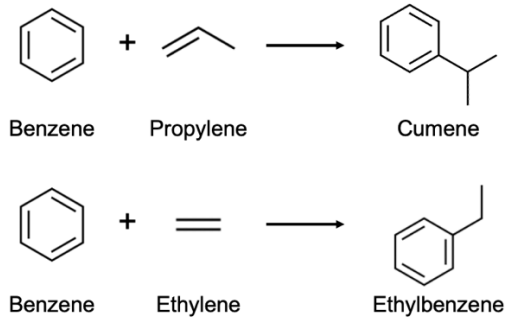

Figure 1.1 Benzene alkylation with propylene and ethylene to form cumene and ethylbenzene.

1.2 Acidic Zeolites for Benzene Alkylation Catalysis

Zeolites have been used as solid acid catalysts to synthesize fuels and fine chemicals due to their ordered microporous networks, low production costs, and mechanical and thermal stability.[2,8,9] Zeolites are well-defined aluminosilicate crystalline structures that consist of pores and channels that vary in molecular dimensions. Their unique microporous structures and resulting molecular shape selectivity have made them popular as catalysts and molecular sieves since the 1960s.[8] Zeolites are comprised of tetrahedra with a central T atom (typically Si, Al, P, etc) linked by oxygen atoms resulting in a three-dimensional crystalline structure seen in figure 1.2.[1,10]

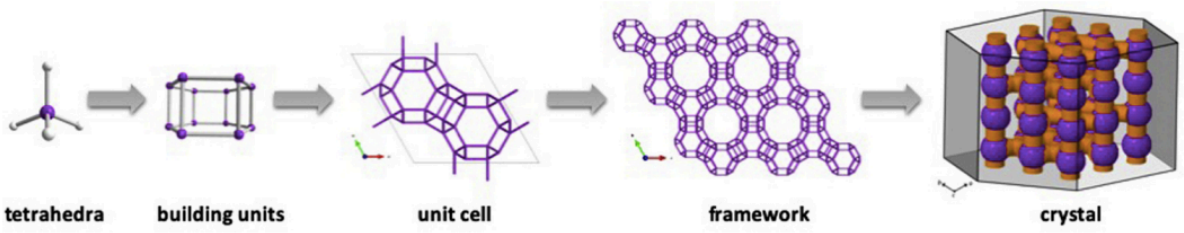

Figure 1.2 Schematic representation of zeolite structure formation.[1]

Pure silica tetrahedra is electrically neutral; however, replacement of the Si atom with an Al atom at the central T atom produces a tetrahedra with a negative charge. To balance this negative charge in the framework, a charge-balancing cation (H^+, Na^+, K^+) is required.[1,2] When the charge balancing cation is a proton, the bridging hydroxyl group acts as a Brønsted acid sites (BAS) capable of mediating chemical reactions in alkylation, isomerization, and cracking processes.[2,11] Different tetrahedra connections and ratios lead to a variety of frameworks resulting in different ring sizes and pore dimensions. Over two hundred natural and synthetic zeolites have been

identified and been assigned a three-letter code by the International Zeolite Association.[2] Figure 1.3 shows some of the widely used zeolites for benzene alkylation with their respective framework and pore sizes.

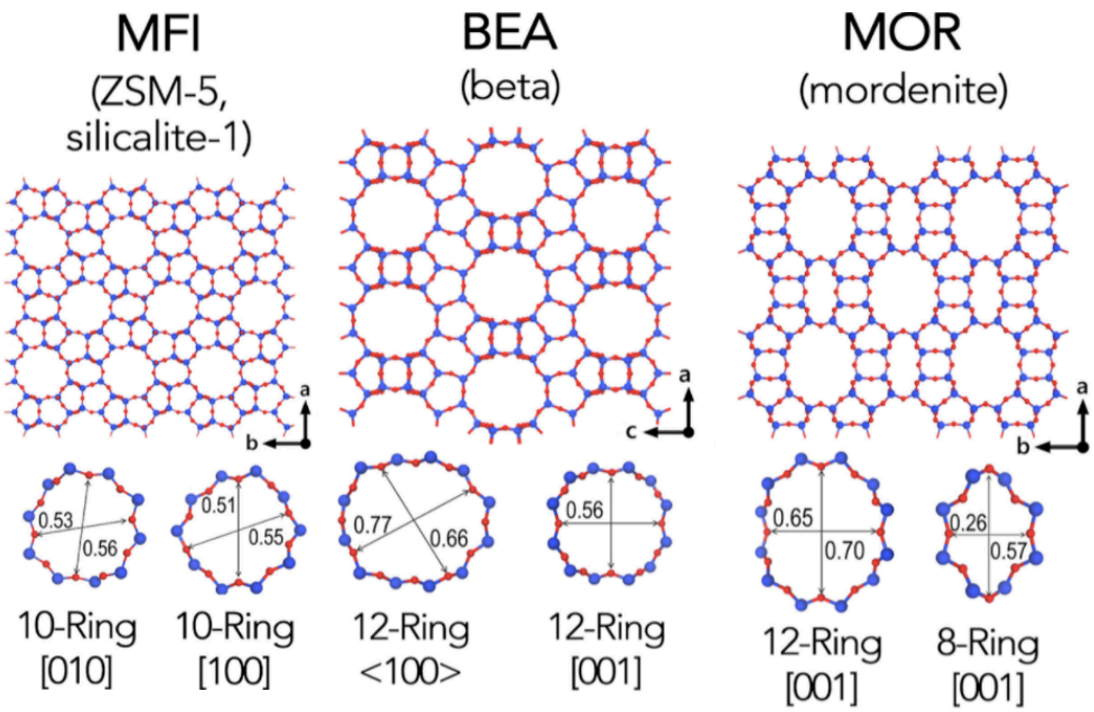

Figure 1.3 Widely used zeolite framework types.[2]

In addition to BAS, the microporous structure of zeolites can provide stability for reactants as well as transition states of desired products through confinement within the pore. Confinement within zeolites can be referred to as the interactions between the host, zeolite framework, and the guest, reactant molecules.[12,13] This interaction exists in many catalytic systems including enzyme catalysis, heterogeneous catalysis, and homogeneous catalysis.[12] Confinement within the pore can mediate different reaction pathways as the extent to which the reaction takes place depends primarily on the contact between the molecule and pore wall and the strength of the van der

Waals interactions which is determined by the chemical identity of atoms/functional groups in the reactant and their distance from the oxygens within the pore framework.[14] A reaction can result in several products with varying structures and dimensions; however, specific product formation may be inhibited if their corresponding transition state size does fit within the pore.[15] Thus, the catalytic performance of a zeolite depends on the size of the micropore in relation to the size of the reactants, intermediates, and relevant transition states.[5] However, there is very little research in understanding how the microporous structure surrounding the active sites of zeolites influences reaction stability and selectivity.

Industrially, zeolite catalysts (like MOR, MWW, BEA, and MFI) have been used in benzene alkylation due to their well-defined microporous structure, no-corrosive nature, and environmentally friendly behavior compared to traditional acid catalysts like $AlCl_3$ and SPA.[10,16,17] Primary concerns for zeolites in industrial processes are catalyst deactivation and downstream product separation. Due to the rigid structure and size of the pores and channels, the formation of bulkier products and byproducts can block the channels and active sites leading to deactivation. For this reason, commercial benzene alkylation with zeolites typically utilizes high benzene to alkene ratios (2-8) to mitigate alkene oligomerization as bound propylene readily dimerizes causing coke formation and subsequent catalyst deactivation.[4,18,19] Typically, recovery and recirculation of benzene is also required which can be energy intensive and costly; therefore, developing catalysts that can operate at a lower ratio can improve process performance.

Understanding the role of Brønsted acid sites in catalyst deactivation is also important as zeolite performance is heavily dictated by the location and distribution of active sites within the microporous structure.[20] There are currently two suggested pathways for benzene alkylation on zeolites, a concerted and a stepwise seen in Scheme 1.1.[17] In the concerted pathway, alkene

protonation and benzene alkylation occur simultaneously via an Eley–Rideal type mechanism where a π-bonded alkene reacts with a weakly-bound benzene to form an alkylated product. The stepwise mechanism, however, occurs when alkene protonation and benzene alkylation occur sequentially. In this mechanism, a π -bonded alkene reacts with the H^+ to form an alkoxide intermediate, which then reacts with a weakly bound benzene to form an alkylated product. Both pathways have been highly debated in literature with evidence showing the plausibility of each pathway.

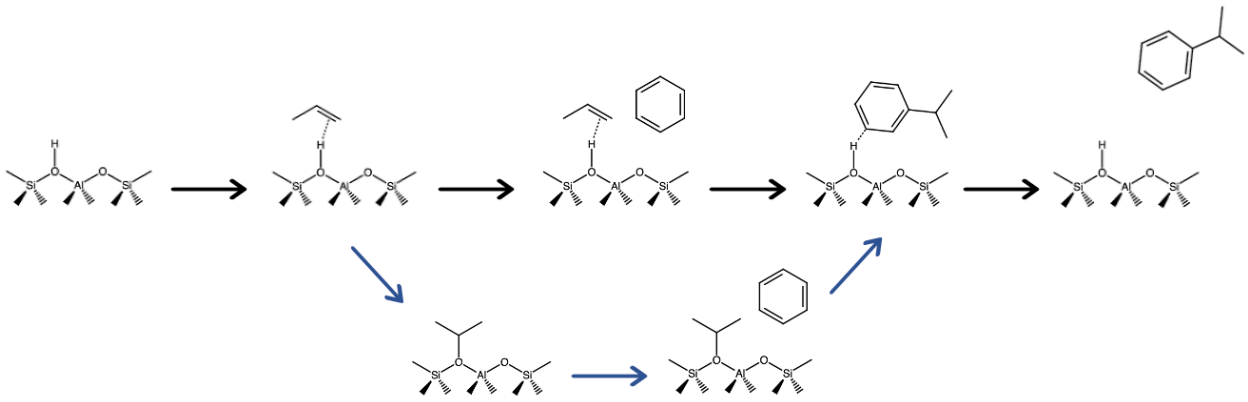

Scheme 1.1 Sequence of elementary steps for benzene alkylation with propylene on acidic zeolites via the stepwise and concerted pathway

1.3 Infrared Spectroscopy for Brønsted Acid Site Analysis

Infrared spectroscopy (IR) can be utilized to characterize the protons of MOR as well as provide insight into the mechanism of bound reactant species. In particular, IR can be used to identify the reaction pathway for benzene alkylation by determining the type of bond formed when reactants are introduced. Infrared spectroscopy can also offer information on the BAS of the zeolite by focusing on the 3800-3000 cm^{-1} region which corresponds to the OH stretching vibrations.[1] There are two bands within the OH stretching frequency region of MOR, one at

~3745 cm^{-1} associated with silanol groups and one at ~3610 cm^{-1} associated with BAS.[16] The asymmetrical shape of the band at ~3610 cm^{-1} has previously been identified as two overlapping signals with a high-frequency signal ~3610 cm^{-1} indicative of BAS in the 12-MR and a low-frequency signal ~3590 cm^{-1} indicative of BAS in the 8-MR.[16,21,22] Deconvolution of the asymmetric band at ~ 3610 cm^{-1} can provide the relative concentrations of the BAS in the 8-MR and 12-MR respectively.

1.4 Computational Modeling Using Density Functional Theory

In more recent years, theoretical models have been used along with experimental data to analyze the interaction of reactants, intermediates, and products with zeolite active sites as well as identify the structures and free energies of associated transition states. Quantum chemical methods like density functional theory (DFT) can be used to compute vibrational frequencies of stable reaction intermediates and allow direct comparison to spectroscopic data.[4] DFT calculations can also be used to determine optimized configurations of stable intermediates and transition states adsorbed onto the Brønsted acid site, which can in turn be used to identify minimum energy reaction pathways.[23] DFT results can aid in reaction engineering by providing expected transition states for each possible pathway allowing the ability to tune the pore dimensions to fit that of the desired products transition state.E.20[14]

1.5 Outline of Thesis

This work aims to combine kinetic, spectroscopic, and theoretical methods to identify the reaction pathway and understand the impact that the microporous structure of MOR has on the reactivity, selectivity, and stability for aromatic alkylation. Chapter 2 provides detailed information about reactor design and development along with key safety features for high

pressure, high temperature reactor systems. The reactor system was designed and built during the thesis work. In this work, we take toluene alkylation on MOR as our model system to avoid the handling of toxic benzene but maintaining similar reaction schemes to benzene alkylation while providing additional information on isomer product formation. In Chapter 3, we discuss how selective titration of protons from the 8-MR in MOR impacts the stability and selectivity for toluene alkylation to desired products. We show that selective titration of protons in the 8-MR results in improved stability for toluene alkylation on MOR. We additionally look at the reaction pathway for toluene alkylation using kinetic and spectroscopic techniques and find that the protons are saturated with π-bonded toluene that reacts with ethylene to form ethyltoluene. Chapter 4 summarized the main conclusions in this thesis and discusses the future direction of this work.

CHAPTER 2

REACTOR DESIGN AND DEVELOPMENT

2.1 Reactor Design

Benzene alkylation is typically performed at high temperatures and pressures. For this reason, a stainless-steel system was constructed to carry out reactions at these operating conditions. Catalytic reactions of toluene and ethylene were carried out in a packed bed 316 stainless steel tube reactor (6.6mm ID, 31.4 cm long). Reactor heating was done with a ATS series 3210 tube furnace and a Watlow EZ-ZONE PM controller. The reactor was loaded with 0.2 g mordenite (60-80 mesh), and 2 g of acid washed silica sand (Supelco) acting as an inert material. A quartz rod (6 mm diameter, 18 cm long) was inserted in the reactor prior to catalyst loading with a layer of quartz wool both above and below the catalyst. This was done to ensure the catalyst bed was at the center of the stainless-steel reactor. A 316 SS thermocouple probe was inserted into the top of the reactor and pushed down until it reached the catalyst bed so that accurate reaction temperature could be recorded. The reactor loading scheme can be seen in Figure 2.1.

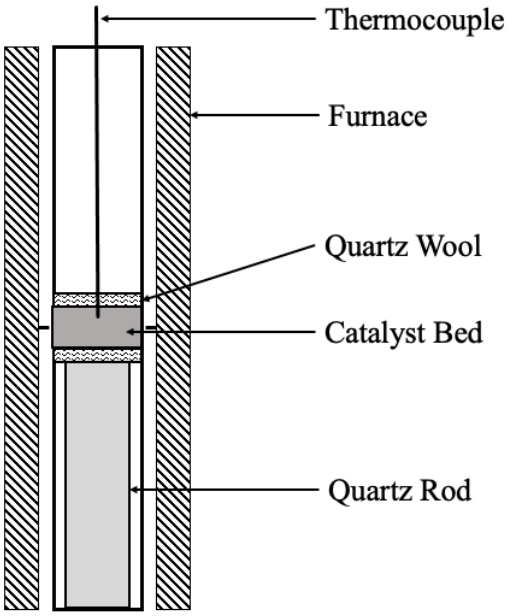

Figure 2.1 Schematic diagram of packed bed reactor

Once loaded, the reactor was pretreated under flowing air at 673 K at a ramp rate of 0.167 K s^{-1} then held for 1 hour to purge any moisture/bound species and subsequently cooled under helium to 473K. The system pressure was controlled using a TESCOM back pressure regulator. The reactor was pressurized then leak checked before each experiment to check for wear down of the threading with replacement as needed. Once the reactor was stabilized to the desired pressure under helium, the system was switched to the bypass line in order to pressurize and stabilize the reactants before introduction into the reactor.

Helium, air, and ethylene were controlled using Parker Porter Series II mass flow controllers. Helium was used as a carrier gas. Calibration of the mass flow controllers was performed using a Restek flowmeter. Toluene flow rates were controlled using a Teledyne ISCO 500D syringe pump. A pressure vessel filled with quartz wool acted as a vaporizer to convert toluene into a gas phase. All lines after the introduction of toluene into the system were kept at 373-393 K. Toluene

partial pressure was also kept below the vapor pressure of toluene at 1 MPa to prevent liquid formation. Ratios of toluene to ethylene were varied from 5:1 to 2:1 with total flows of 100 sccm.

An Agilent 6890 gas chromatograph equipped with a capillary HP-1 Agilent column (50 m x 320 μm x 1.05 μm) and flame ionization detector (FID) was used to analyze the effluent. Calibration curves for ethylene, methane, and propylene were generated using gas standards while the toluene calibration curve was done using liquid toluene balanced with helium gas. Reactants were stabilized under a bypass loop for several GC injections before introduction into the reactor. The effective carbon number was used to estimate concentrations of unknown products.

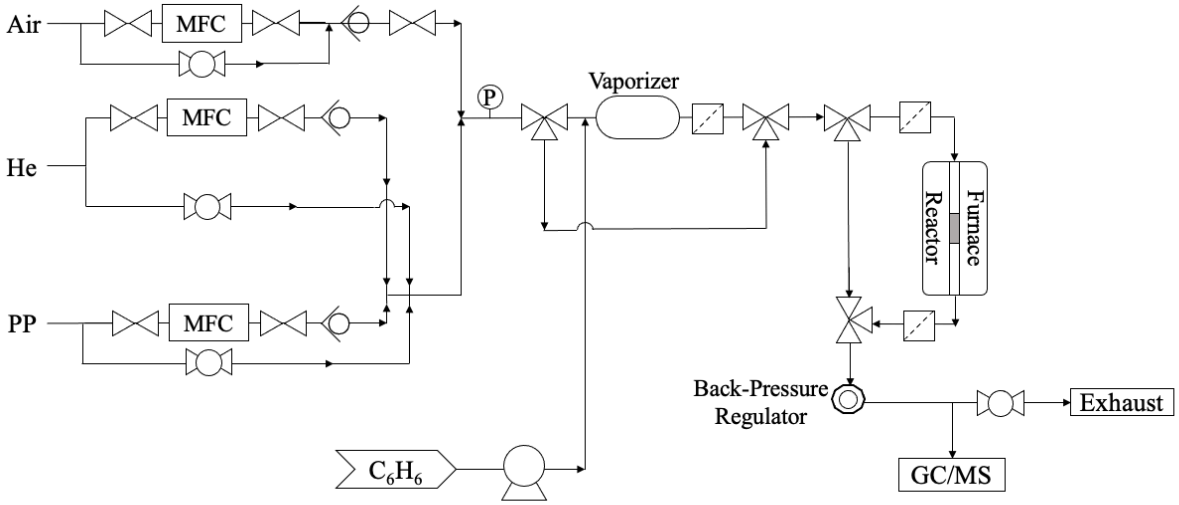

Figure 2.2. Schematic of reactor setup

2.2 Reactor Safety Features

Operating at high temperatures and pressures requires additional safety features such as a pressure relief valve or way of regulating the pressure so that it does not result in a runaway reaction. In this system, there are several safety features in place. The primary one is the mass flow controllers which are controlled using online software and will stop flow if the outlet pressure is higher than the inlet pressure reducing the risk of over pressurization. In order for the mass flow controller shut off to work successfully, the gas tank regulators must be set to a value that is higher than the reaction pressure to provide a pressure difference. The mass flow controllers in conjunction with the gas tank regulators, which only provide pressure that is 0.5 MPa above operating pressures, can reduce the risk of over pressurizing the system. In addition to pressure regulation, the furnace has a high temperature limit of 873 K in which the furnace will shut down if this temperature is exceeded. The entire system is located within a walk-in hood for further safety against exposure to toluene and ethylene gases.

CHAPTER 3

TOLUENE ALKYLATION WITH LIGHT ALKENES ON ACIDIC MORDENITE ZEOLITE: THE EFFECTS OF ACID SITE LOCATIONS AND CONFINEMENT ON REACTION MECHANISMS

Paper in preparation

Hanna Monroe[1], Michelle Nolen[1,2], Kemakorn Ithisuphalap[1], Stephanie Kwon[1*]

3.1 Abstract

Aromatic alkylation with ethylene and propylene are important reactions to produce cumene and ethylbenzene. Acidic zeolites are widely used in the petrochemical industry due to their high reactivity, non-corrosivity, and environmentally friendly nature compared to traditional liquid acids. Yet, the reaction pathways of benzene alkylation on solid acids have remained uncertain. Moreover, the role of microporous structure in zeolites in reactivity, selectivity, and stability for benzene alkylation pathways has remained unclear. This work combines kinetic, spectroscopic, and theoretical methods to identify the reaction pathways and to understand how the microporous structure impacts the reactivity and stability, taking the toluene-ethylene reaction as a model reaction.

---

[1] Colorado School of Mines, Golden, CO, 80401

[2] National Renewable Energy Laboratory (NREL), Golden, CO 80401

* *Corresponding author: kwon@mines.edu*

In doing so, we show that exchanging H^+ sites in the 8-membered ring (8-MR) significantly improves the stability of acidic mordenite zeolites by lowering the contribution of alkene dimerization reactions that lead to coke formation. Detailed in-situ infrared spectra show that protons are saturated with π-bonded toluene, which sequentially react with ethylene to form ethyl toluene. These results can be utilized to provide design strategies for solid acid catalysts used in benzene alkylation with improved stability, selectivity, and reactivity.

3.2 Introduction

Alkylation of aromatics, such as benzene and toluene, with ethylene and propylene is a key reaction in the petrochemical industry to produce cumene, ethylbenzene, and ethyl toluene. These chemicals are important intermediate products to form phenol, styrene, and acetone, which are used to make commodity products including polystyrene, polycarbonate, and phenolic resins.[3–6] Acidic zeolite catalysts have been utilized for benzene alkylation due to their well-defined microporous structure, non-corrosive nature, and environmentally friendly behavior compared to traditional acid catalysts, such as $AlCl_3$ and solid phosphorous acid.[16,17] Commercial benzene alkylation reactions are typically operated at high benzene to alkene ratios (2-8) to mitigate alkene dimerization routes, which often lead to catalyst deactivation via coke formation.[18,24,25] Such requirements of high benzene to alkene ratios, in turn, impose additional costs to recover excess benzene downstream. In addition to parallel alkene dimerization reactions, the primary alkylated product can further react to form di- and tri-alkylated products, which require a transalkylation unit to convert them back into desired monoalkylated products.[4] Both of these recovery processes can be energy intensive and costly. Therefore, developing catalysts that can operate at lower aromatic/alkene ratios with high selectivity towards monoalkylated products is highly desired to improve process performance and efficiency.

Conventional benzene alkylation reaction routes on zeolites include concerted and stepwise mechanisms (Scheme 3.1).[11,17,26–28] The concerted pathway involves the direct C-C formation between the π-bonded alkene and toluene via an Eley–Rideal type mechanism. The stepwise mechanism, in contrast, involves the formation of alkoxide intermediate via the protonation of π-bonded alkene, where the alkoxide sequentially reacts with benzene to form alkylated product. Both pathways have been highly debated in literature with results showing the plausibility of each pathway to occur leading to inconclusive results. Previous DFT studies have shown that a concerted pathway is kinetically favorable due to a lower activation energy compared to the stepwise pathway.[10,17] While others, through DFT and molecular dynamics, have concluded that the stepwise pathway via an alkoxide is favorable.[28,29]

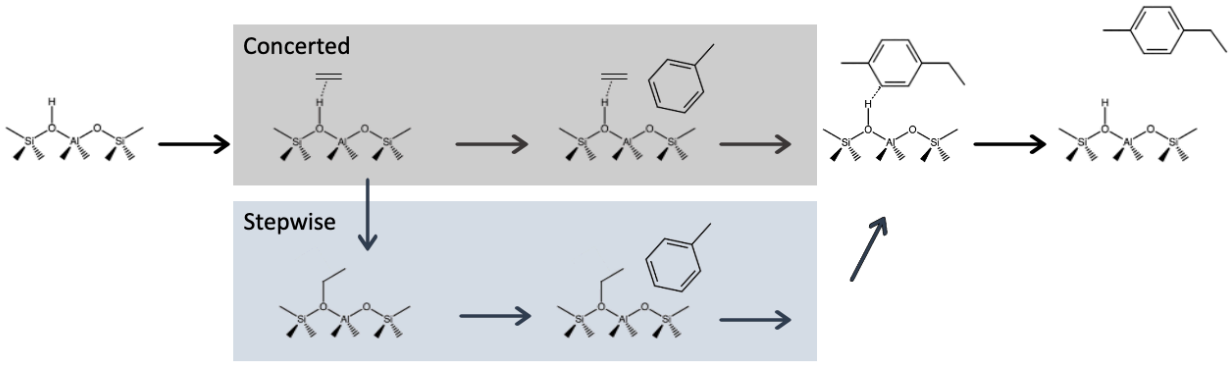

Scheme 3.1 Conventional reaction mechanisms for toluene alkylation with ethylene on acidic zeolites via concerted and stepwise pathways.[27]

Different types of acidic zeolites have been tested for benzene alkylation, including BEA, MOR, MWW, and MFI zeolitic frameworks.[4,30,31] Acidic MOR and MFI zeolites have been implemented industrially since the 1980s for ethylbenzene and cumene production; more recently, however, MWW and BEA zeolites have shown provide improved selectivity and stability.[4,32] Several publications cite BEA as providing higher cumene selectivity with minimal

byproduct formation while others claim MWW had better stability with similar cumene selectivity to BEA. [10,17,30,31] Although, a variety of zeolites have been used for commercial benzene alkylation, there is still a lack of literature aimed at understanding how the microporous structures of zeolitic framework and the locations of acidic H^+ sites impact their catalytic selectivity and stability.

Micropores of molecular dimensions, such as those in microporous zeolitic framework, can provide extra stabilization of the relevant transition states (over their precursors) via van der Waals interactions.[12] Such interactions depend sensitively on the "fit" between the organic molecules (guest) and the confining micropores (host), similar to the lock-and-key concept often employed in enzyme catalysis. Thus, the reactivity of acid H^+ sites within zeolites can depend on their locations and the size and shape of the secondary container that surrounds such acidic sites. Yet, there are only few examples that show how these confinements influence the reaction selectivities and stabilities.

This work combines kinetic, spectroscopic, and theoretical methods to probe mechanistic details of alkylation pathways and the impacts of microporous structures in zeolites on the reactivity, selectivity, and stability of monoalkylated product formation. We focus on toluene alkylation to avoid the use of highly toxic benzene reactants; toluene alkylation catalysis also offers additional information of the C-C formation locations via unique isomer formations, while still exhibiting similar reaction scheme as benzene alkylation. Acidic MOR zeolite is chosen as our model catalyst due to its industrial relevance; it also contains H^+ sites located at two distinct porous environments, offering the ability to study the effects of pore confinement on the catalytic activity, selectivity, and stability. In doing so, we show that selective titrations of H^+ sites in 8-membered ring (MR) via Na^+ exchange methods significantly improve the stability of toluene

alkylation on MOR. Kinetic and spectroscopic methods were combined to show that the H+ sites are saturated with π-bonded toluene, which reacts with ethylene to form ethyl toluene products. These results can be utilized to aid in catalyst design strategies to improve catalytic performance by providing insight into how the microporous structure can be tuned to fit the transition state of the desired product leading to improved selectivity.

3.3 Methods

3.3.1. Catalyst Synthesis and Treatment Protocols

MOR was purchased commercially from Zeolyst in its ammonium cation form with a Si/Al ratio of 10. To convert MOR to its protonated form (H^+-MOR) and remove ammonia and any ambient moisture, the sample was pretreated in flowing air (2.5 $cm^3\ g^{-1}\ s^{-1}$, 99.999%, VWR zero air generator) at 773 K with a ramp rate of 0.0167 K s^{-1} and holding for 4 hours.

H^+-MOR samples were exchanged using $NaNO_3$ solutions at varying molar concentrations (0.5M to 3M). the exchange was performed in a round bottom flask where 1 g of catalyst was stirred in the $NaNO_3$ solution at 353 K for 12 h using an oil bath. The solution was centrifuged at 3000 rpm for 5 min followed by liquid decanting. The exchanged sample (Na^+-MOR) was rinsed, centrifuged then decanted several times and dried at 353 K in an oven for 12 h. Once dry, the sample was sieved to achieve particles within 180-250 μm. The sample was calcinated again at 773 K at a ramp rate of 0.0167 K s^{-1} in flowing air (2.5 $cm^3\ g^{-1}\ s^{-1}$, 99.999%, VWR zero air generator) and holding for 4 hours.

3.3.2. Catalytic Measurements

Alkylation rates were measured on MOR samples (180-250 μm) in a packed bed 316 stainless steel tube reactor (6.6mm ID, 31.4 cm long). MOR samples (0.2-0.6 g) were mixed with 2 g acid washed silica sand (Supelco) to increase catalyst bed height. Silica sand did not show

alkylation product formation when tested at reaction conditions. Samples were pretreated by heating to 673K under flowing air at 0.167 K s^{-1} for 1 hour to remove any bound ambient moisture then cooling under helium to the desired reaction temperatures.

Mass flow controllers (Parker Porter, Series II) were used to control and maintain desired inlet flow rates for helium (99.999%, General Air), air (99.999%, VWR zero air generator), and ethylene (99.9%, General Air). Toluene (99.5%, Fisher Chemical) flow rate was controlled using a syringe pump (Teledyne ISCO 500D). All lines after the introduction of toluene into the system were kept at 373-393 K to prevent condensation within the lines. Catalyst bed temperatures were maintained using an electric tube furnace (ATS, Series 3210) and a temperature controller (Watlow EZ-ZONE PM) and measured using a thermocouple (K-type, Omega) inserted into the reactor until it was touching the catalyst bed. A back pressure regulator (TESCOM) was used to control and maintain reaction pressure requirements. Reactant and product concentrations were analyzed using gas chromatography (Agilent, 6890) equipped with a capillary HP-1 Agilent column (50 m x 320 μm x 1.05 μm) and a flame ionization detector (FID) as well as mass spectrometry to confirm product identity.

3.3.3. Infrared Assessments

Infrared spectra were collected in transmission mode using a Nicolet iS50 FT-IR (Thermo Fisher) spectrometer. MOR samples were pressed into a self-supporting wafer (~10-30 mg) then loaded into a stainless-steel, high temperature cell (Harrick Scientific Products) fitted with NaCl windows. Cell temperature was controlled using an electronic controller (Harrick Scientific Products, ATK-024) with a thermocouple (K-type, Omega) inserted through the cell to touch the outer side of the wafer and cooling from a chiller (Neslab Coolflow CFT-25).

MOR wafers were first pretreated by heating to 673K under air at 0.167 K s^{-1}, holding for 1 hour, then cooling under helium to desired reaction temperatures. Spectra were taken during pretreatment to ensure that any bound species from exposure to ambient conditions when loading were removed. Gas reactant flow rates were controlled using mass flow controllers with a syringe pump (KD Scientific series 200) for liquid toluene. Line temperatures were maintained using resistive heating at 373-393 K. All spectra were collected over 64 scans at a resolution of 4 cm^{-1} from 4000-400 cm^{-1}.

In addition, infrared spectra was used to determine the relative concentration of Brønsted acid sites between the 8-MR and 12-MR from the intensity of the asymmetric OH stretching region (3550-3650 cm^{-1}).[22] Previous studies have shown that the asymmetric nature of the OH region is due to a high and low frequency band which can be deconvoluted into two bands indicative of protons within the 8-MR and 12-MR residing at ~3590 cm^{-1} and ~3610 cm^{-1} respectively.[21,22] In this work, Origin software was used to deconvolute the OH stretching region using multiple peak fit. Brønsted acid site distribution was calculated based on the integrated areas of the individual bands for the 8-MR and 12-MR on H^+-MOR and Na^+-MOR samples.

Infrared spectroscopy was additionally used to gain insight into the identity and surface coverage of bound species during toluene alkylation. The change of intensity in the OH stretching region was monitored after the introduction of reactants at varying pressures to determine the most abundant surface species and associated equilibrium constants. Surface coverage (θ_A) was calculated using Equation 3.1.

$$\theta_A = \frac{K_{eq} \cdot P_A}{1 + K_{eq} \cdot P_A} \tag{3.1}$$

where P_A is the partial pressure of the reactant and K_{eq} is the equilibrium constant. Equilibrium constants were calculated for reactants on both H^+-MOR and Na^+-MOR samples and compared to DFT-derived free energies.

3.3.4. Computational Methods – Density Functional Theory

All density functional theory (DFT) calculations were performed with Vienna Ab initio Simulation Package (VASP) to determine structures, identify transition states, and extract thermodynamic quantities.[33,34] The generalized gradient approximation (GGA) with the revised Perdew Burke Ernzerhoff (RPBE) functional was used to approximate the exchange-correlation energy functional.[35] The DFT-D3 method of Grimme was applied to account for dispersion forces.[36] Electron-ion interactions were described using the projector augmented-wave method with electronic wave functions expanded in a plane-wave basis set with a kinetic energy cutoff of 396 eV. The electronic convergence criterion was set to 10^{-6} eV between successive electronic relaxation steps, while ionic convergence was set to occur when the Hellman-Feynman forces acting upon each atom fell below 0.05 eV/Å. The MOR systems were modelled with a 1×1×1 Monkhorst-Pack k-point mesh of the Brillouin zone.

Two-unit cells in the z – direction of the MOR framework were used to avoid interaction among neighboring acidic T-sites and adsorbates. This yields a Si:Al ratio of ~100, representative of dilute experimental conditions (Si:Al = 10). For each T-site, the four oxygen atoms were probed to find the optimal proton location, which was taken to be the location with the lowest electronic energy. Figure 3.1 shows possible T-site and proton locations for MOR framework.

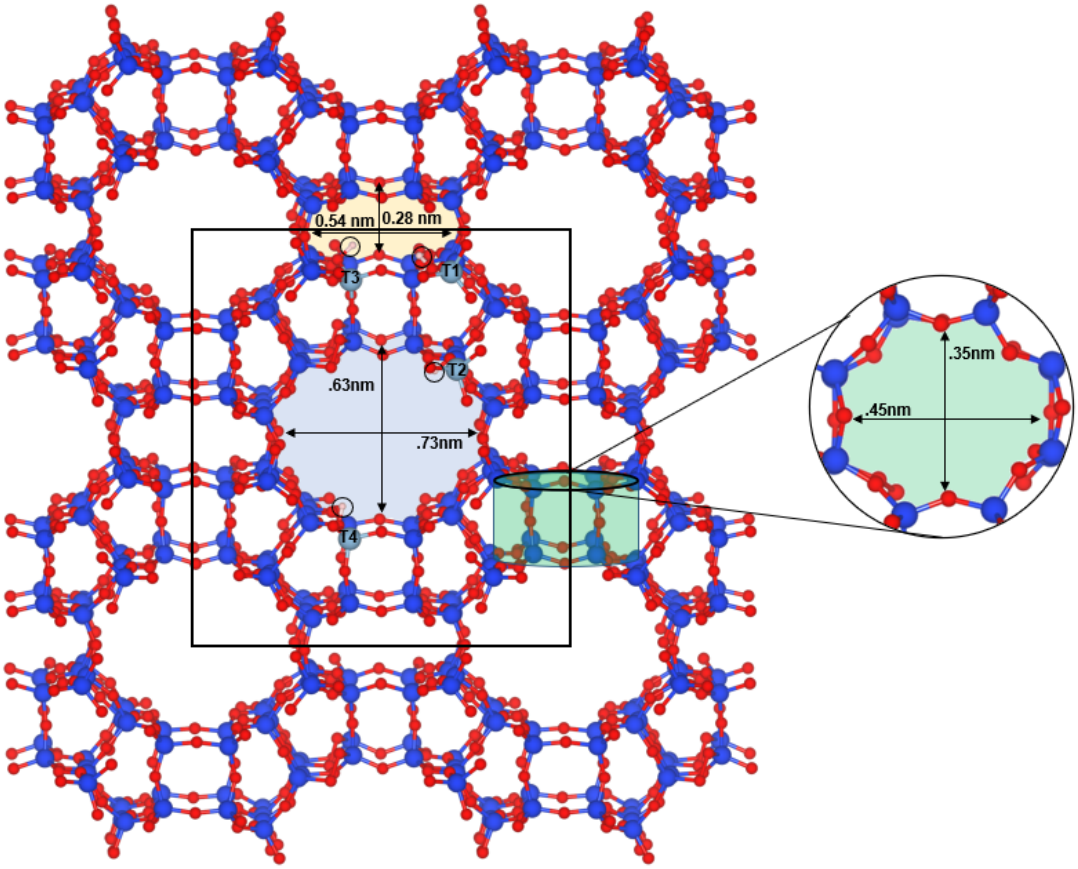

Figure 3.1 Crystallographic structure of MOR framework with possible T-sites and H^+ locations. The unit cell is shown in black line. Magnification shows the side channel (green) connecting 8MR (yellow) and 12MR (blue).

Geometry optimization calculations were performed for each adsorbate by relaxing the unit cell of protonated mordenite (H^+-MOR) with the adsorbate for a minimum of ten permutations, with starting geometries derived from previous DFT adsorption studies of zeolite systems in the literature.[11,26,37–39] The global minimum electronic energy of these permutations was taken to be the optimal geometry of the adsorbate. Multiple proton locations were tested with each adsorbate configuration at a given T-site. Adsorption energies of propylene, isopropoxide, ethylene, ethoxide, benzene, and toluene were consistently most favorable (exothermic) in T1 sites in the 8MR and T2 sites in the 12MR. Therefore, T1 and T2 were

chosen to represent energetics in the 8MR and 12MR, respectively; only energetics calculated at these two T-sites are discussed here. The adsorption energy of each species was calculated by:

$$\Delta E_{ads} = E_{\text{adsorbed species}} - (E_{\text{H+-MOR}} + E_{\text{gas phase}}) \quad (3.2)$$

where $E_{\text{adsorbed species}}$ is the total DFT-derived electronic energy of the species and surface, $E_{\text{H-MOR}}$ is the energy of the MOR framework with the relevant T-site (T1 or T2), and $E_{\text{gas phase}}$ is the energy of the adsorbate in the gas phase; E_{ads} is resultant the adsorption energy. Alkoxide adsorption energies were taken with respect to their gas-phase alkene. The use of the D3 dispersion correction permits the total energy of a system to be separated into the van der Waals (vdW) and quantum mechanical energies:

$$E_{\text{TOTAL}} = E_{\text{QM}} + E_{\text{vdW}} \quad , \quad (3.3)$$

where E_{total} is the total DFT-derived energy of the system, *EvdW* is the vdW energy contribution, and E_{QM} is the energy of the system without dispersion forces.

3.4 Results and Discussion

3.4.1. Effects of Micropore Environments on Toluene Alkylation Stability and Selectivity

3.4.1.1. Selective Titration of Protons from the 8-MR

In this work, selective titration was used to control the distribution of protons within each pore to examine the contribution that pore dimensions have on catalyst stability and selectivity for toluene alkylation on MOR. Selective titration of protons from the 8-MR has been previously studied on MOR by Gounder et al attributing this phenomenon to the more electropositive Na^+ cation which appears to be better stabilized by stronger dispersive forces in the tighter confinement of the 8-MR.[22] To determine the extent of sodium exchange, infrared spectra of the OH stretching band was deconvoluted into two distinct bands. For the unexchanged H^+-MOR

sample, deconvolution of the OH stretching region ~3600 cm^{-1} identified the band positions of the 12-MR to be ~3610 cm^{-1} and the 8-MR to be ~3595 cm^{-1} consistent with previous literature values.[21,22] The relative percentage of protons within the unexchanged H^+-MOR sample was determined to be 77% in the 8-MR and 23% in the 12-MR as seen in Figure 3.2.

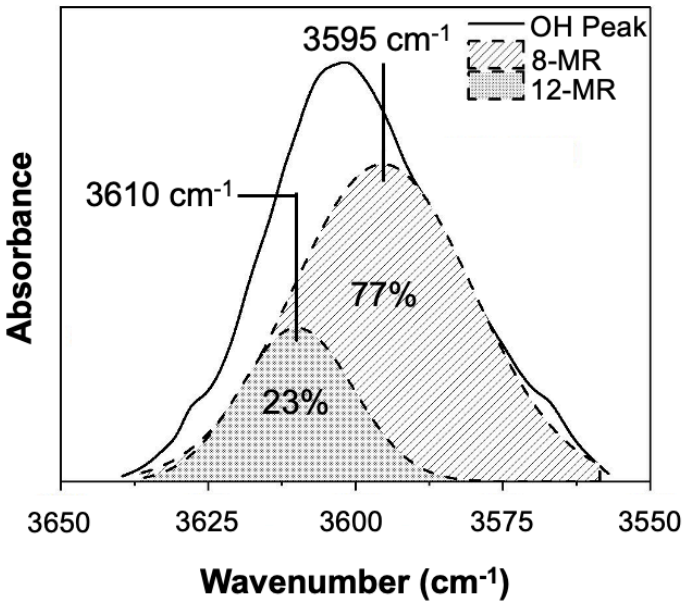

Figure 3.2 Deconvoluted infrared spectra of H^+-MOR (OH region) with relative percentages of protons located in 8-MR and 12-MR.

Deconvolution was additionally applied to MOR samples after sodium exchange. Sodium exchange experiments were carried out using varying molar concentrations (0.5-3M) of $NaNO_3$. Samples are identified by the molar concentration used to perform the catalyst synthesis. Figure 3.3 shows the relative percentage of protons in the 8-MR and 12-MR at varying extents of sodium exchange from deconvolution of the OH region.

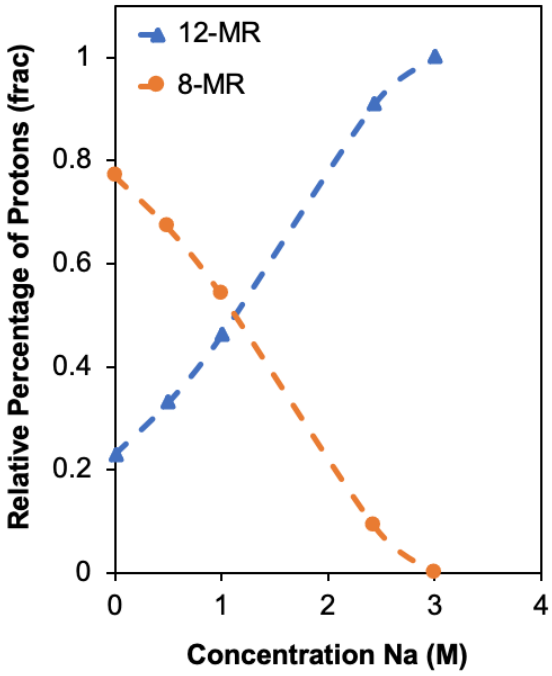

Figure 3.3 Relative percentage of protons in 8-MR and 12-MR of MOR with varying Na^+ determined by deconvolution of OH region.

The relative percentage of protons within the 8-MR diminishes as the molar concentration of sodium solution increases leading to a sample with no protons left within the 8-MR. The 3M $NaNO_3$ solution resulted in complete substitution of protons within the 8-MR. This sample was utilized for further kinetic experiments as a fully exchanged sample that was compared to the unexchanged H^+- MOR sample.

3.4.1.2. Stability and Selectivity Through Selective Titration

To determine the impact of selective titration on MOR catalyst stability, kinetic experiments using a stainless-steel packed bed reactor were performed on both the H^+- MOR and the 3M Na^+- MOR. Identical reaction conditions were run on each sample between 6-16 h taking gas chromatography measurements every 0.5 h. Figure 3.4 shows the turnover rates as a function

of time on stream. Here we show that H^+- MOR deactivates quickly with complete deactivation after 4 hours. 3M Na^+- MOR on the other hand remains stable over the same time period with a minor decrease after 7.5 hours on stream.

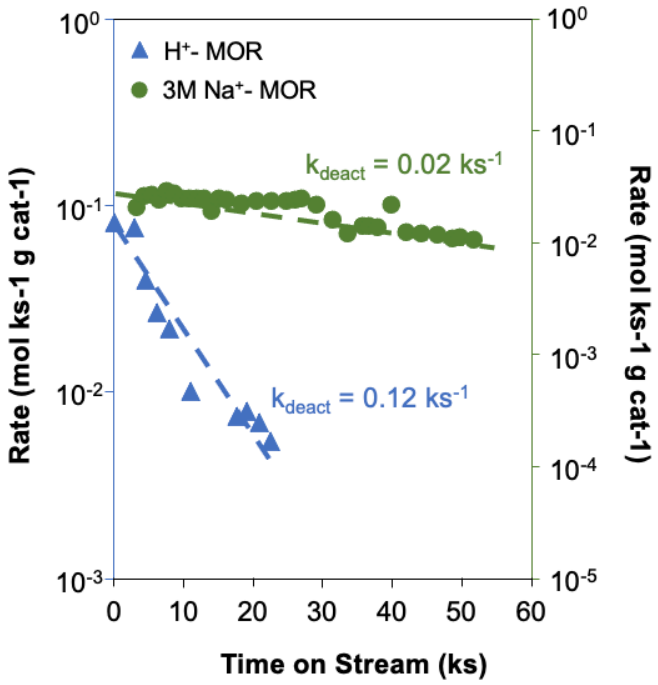

Figure 3.4 Toluene alkylation product formation rates as a function of time on stream for H^+- MOR and 3M Na^+- MOR. Reaction conditions: total pressure of 0.5 MPa at 503K with toluene partial pressure of 50 kPa and ethylene partial pressure of 25 kPa.

Deactivation rate constants were calculated for both samples with H^+- MOR resulting in a 6-fold increase in the deactivation rate constant compared to 3M Na^+- MOR, 0.12 ks^{-1} and 0.02 ks^{-1} respectively. This decrease in deactivation sugguests that protons within the 8-MR play a major role in the deactivation of MOR for toluene alkylation. Therefore, selectively exchanging protons from the 8-MR greatly improves the stability of MOR for toluene alkylation which allows for

kinetic experiments that can run longer and without extrapolation of rates to zero time due to the lack of initial deactivation present in unexchanged H^+-MOR.

Furthermore, we analyze toluene alkylation using gas chromatography to determine the impact that selective titration of protons out of the 8-MR has on product formation. Previous literature has stated that coke formation from alkene dimerization is the primary cause for catalyst deactivation for zeolites.[18,19,24,25] It has been shown through DFT calculations that due to toluene's large size it is does not reside within the 8-MR. Therefore, it is likely that alkene dimerization product formation occurs within the 8-MR and subsequent exchange of protons out of the 8-MR should result in a reduction of these products. Experiments were carried out at 0.5 MPa and 503K with identical operating conditions of 50 kPa toluene and 25 kPa ethylene. Gas chromatography was utilized to analyze product distribution for both MOR samples. On the 3M Na^+- MOR sample, no alkene dimerized products were present confirming that alkene dimerization occurs within the 8-MR of MOR. These kinetic results show that controlling the distribution of protons among the two different pore sizes can lead to improved stability on MOR and selectivity of desired monoalkylated products.

3.4.2. Understanding the Reaction Mechanism of Toluene Alkylation

3.4.2.1. Reaction Pathway Through Kinetic Measurements

As previously discussed, aromatic alkylation reaction pathways have been highly debated in literature with no consensus on the preferred pathway. Here, we aim to understand how the pore structure dictates the reaction mechanism by combining kinetic, spectroscopic, and theoretical methods to determine reaction mechanism and thus the preferred pathway. First, we examine toluene alkylation rates as a function of reactant partial pressures to determine the reaction order

with respect to each reactant. Kinetic measurements were taken on 3M Na^+- MOR as toluene alkylation occurs within the 12-MR of MOR. Figure 3.5 shows product formation rates as a function of reactant partial pressure.

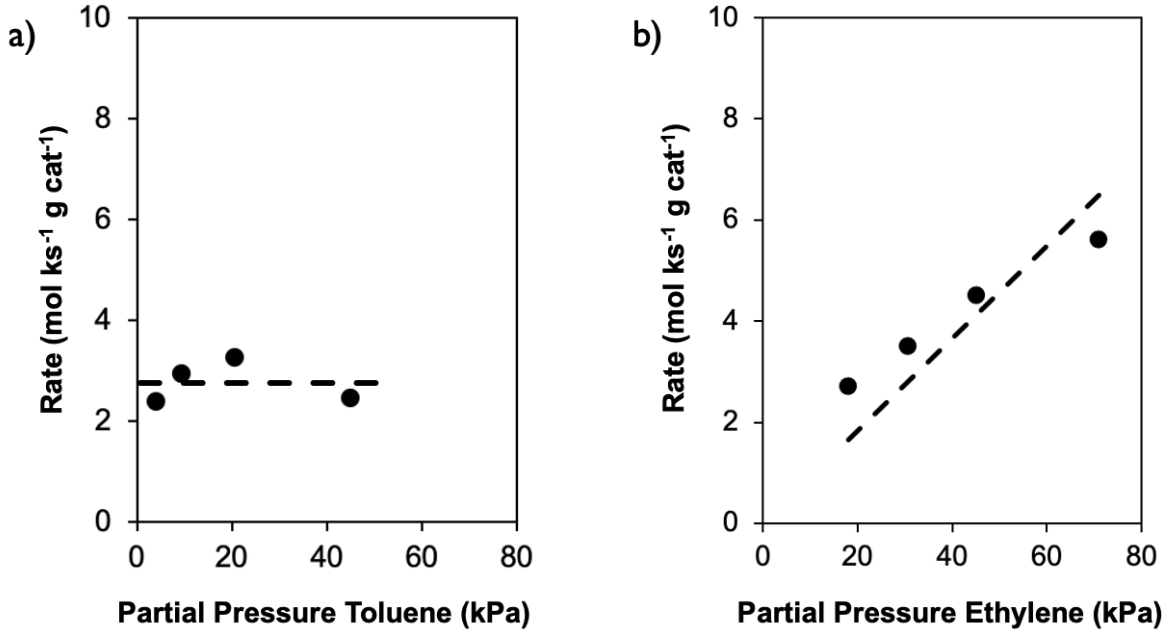

Figure 3.5 Toluene alkylation rates as a function of (a) toluene pressure (5-50 kPa; 25 kPa ethylene) and (b) ethylene pressure (20-75 kPa; 50 kPa toluene) on 3M Na^+- MOR. Reaction conditions: 0.5 MPa and 503K.

As the partial pressure of toluene increased, the rate remained the same leading to a zero order with respect to toluene, meaning that toluene partial pressure has no effect on reaction rates. For ethylene, however, the rate increased linearly with increasing partial pressure leading to a first order with respect to ethylene with linear dependency on the rate. We find that toluene alkylation occurs with a π-bonded toluene that subsequently reacts with gas phase ethylene to form ethyltoluene. Scheme 3.2 shows the elementary steps for a concerted pathway with toluene binding to the proton. A rate equation (Eqn 3.4) can also be derived for this concerted pathway.

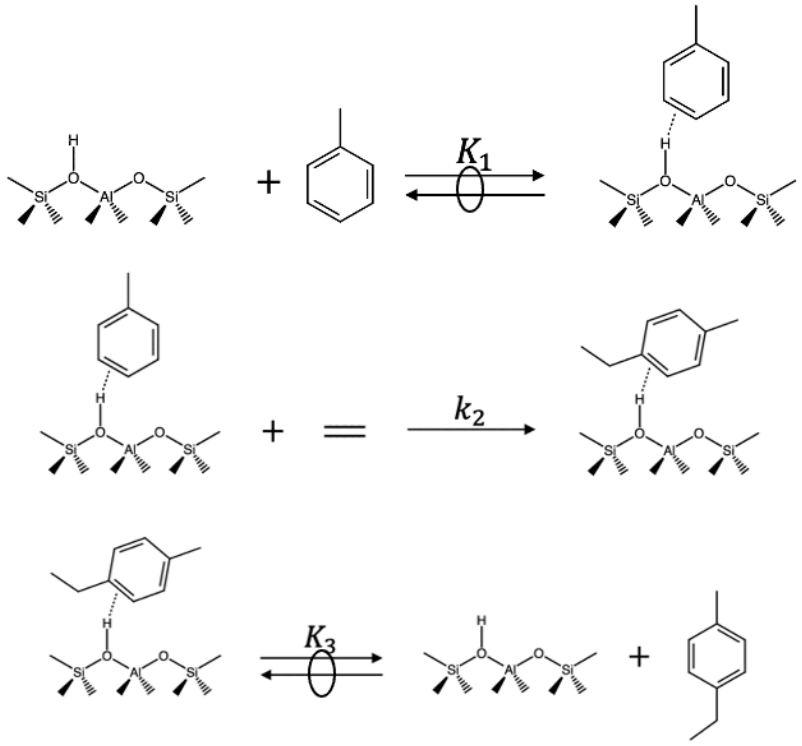

Scheme 3.2 Elementary steps for toluene alkylation following π-bonded toluene

$$r_{concerted} = \frac{k_2 K_1 [C_2H_4][C_7H_8]}{1+K_1[C_7H_8]+K_3[C_9H_{12}]} \quad (3.4)$$

The elementary steps based on kinetic results in this work shown above (Scheme 3.2) differ from both reaction pathways suggested in literature which showed that ethylene covers the surface.[17,26–28] Here we find that toluene is covering the surface following a concerted pathway where the reactant is π-bonded to the proton.

3.4.2.2. Spectroscopic and Theoretical Analysis of the Reaction Mechanism

To probe further into the reaction mechanism, we used infrared spectroscopy to determine the type of bonding and extent of reactant coverage. Figure 3.6 shows the infrared spectra of H^+-MOR before and after the introduction of ethylene. Upon the introduction of ethylene, the OH band decreases in intensity with the appearance of bands between 1500-1450 cm^{-1}, indicative of

a bound ethoxide species (-O-C_nH_{2n+1}).[24,38] Ethylene also has C-H stretching bands around 3300-2800 cm^{-1}. The decrease in OH band intensity without the appearance of broad bands around 2800 cm^{-1}, which are indicative of π-bonding, shows that ethylene is reacting to form an ethoxide.[38]

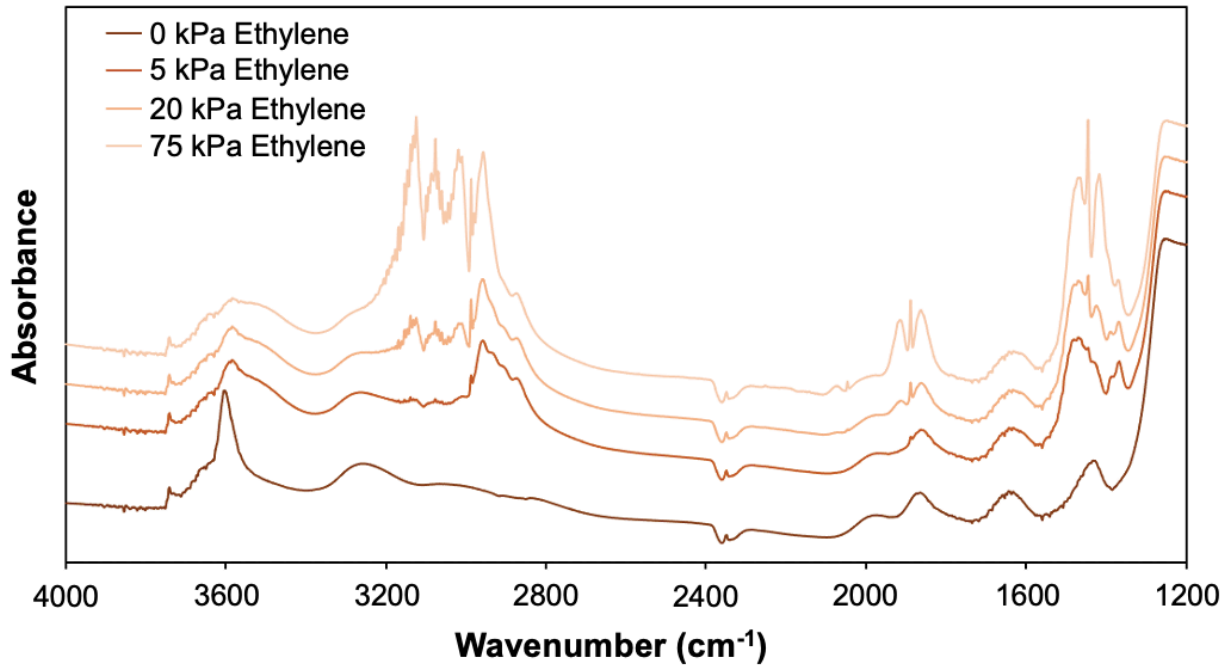

Figure 3.6 Infrared spectra of H^+-MOR in contact with ethylene (0-75 kPa; 473 K).

Propylene has signature bands located in the same regions as ethylene; however, the band shapes are unique. Figure 3.7 shows the infrared spectra of H^+-MOR before and after the introduction of propylene. Upon the introduction of propylene, the OH band decreases in intensity with the appearance of an isopropoxide species (-O-C_nH_{2n+1}) with bands between 1500-1450 cm^{-1}.[24,38] Propylene also has C-H stretching bands around 3300-2800 cm^{-1} similar to

ethylene but with different characteristic bands. Thus, propylene followed the same mechanism as ethylene resulting in a bound alkoxide species.

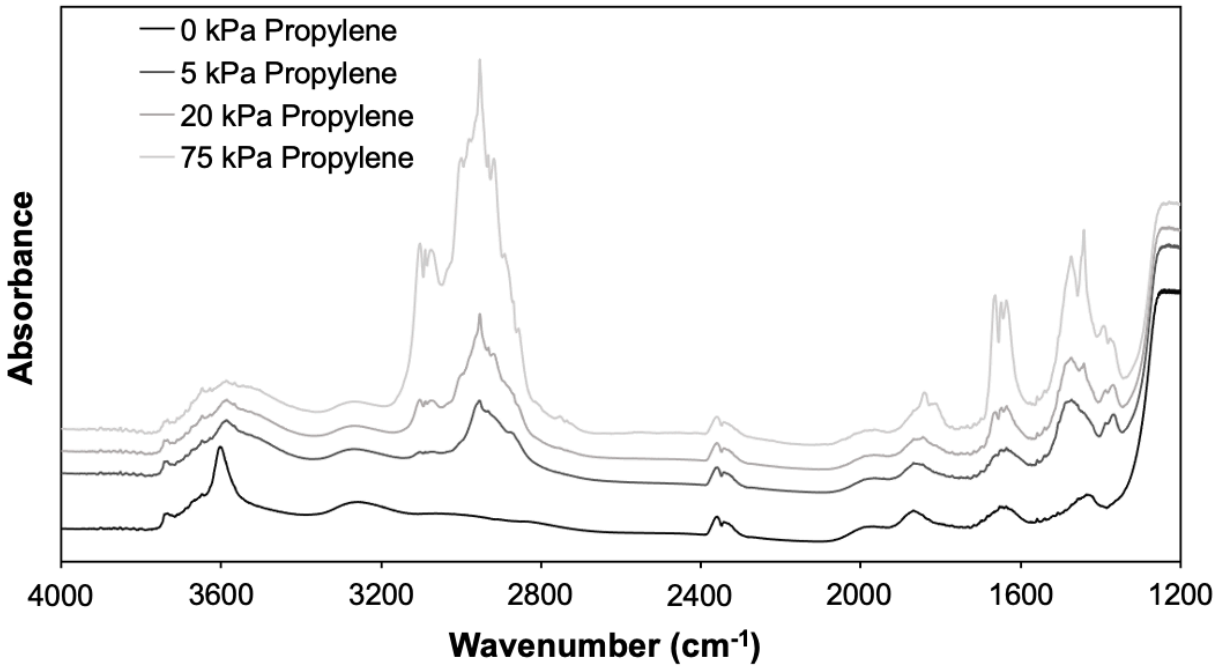

Figure 3.7 Infrared spectra of H^+-MOR in contact with propylene (0-75 kPa; 473 K).

Figure 3.8 shows the full infrared spectra for toluene pressure on unexchanged H^+-MOR. The appearance of toluene's signature bands indicative of C-H stretching at 3300-2800 cm^{-1} and C-C stretching around 1600–1450 cm^{-1} can be seen.[24] The OH stretching band around 3600 cm^{-1} still serves as a means to identify the coverage effects of toluene. When comparing infrared spectra of ethylene and toluene, signature band overlap can be seen between the reactant species as the alkoxide band region (1500-1450 cm^{-1}) overlaps with C-C stretching bands (1600–1450 cm^{-1}) characteristic of toluene making it difficult to determine alkene-proton interactions when

co-feeding. For this reason, infrared spectroscopy measurements were carried out on each reactant individually.

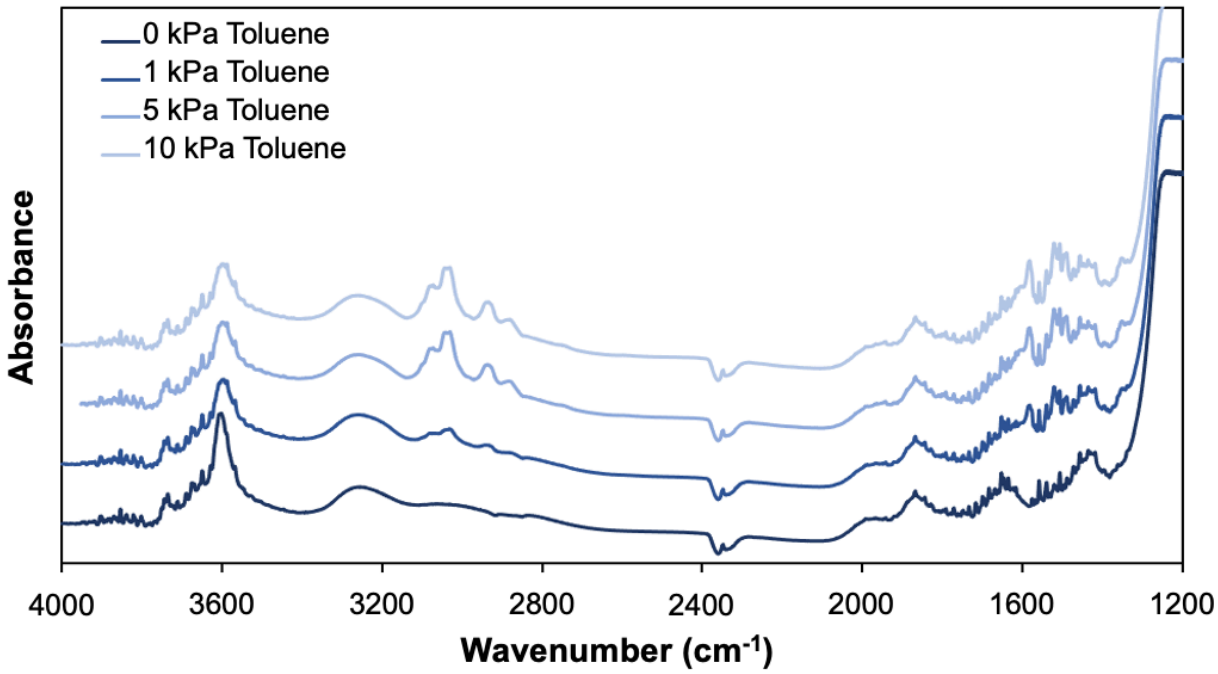

Figure 3.8 Infrared spectra of H^+-MOR in contact with toluene (0-10 kPa; 473 K).

Figure 3.9 compares the OH region for each reactant at increasing partial pressure. Upon increase in partial pressure of ethylene and propylene, the OH band decreases drastically showing the loss of protons and alkoxide formation (Figure 3.9_a and 3.9_b). Infrared spectra of the OH region upon the introduction of toluene shows that, due to toluene's size, it is unable to reach the 8-MR which was confirmed through DFT calculations showing a positive (Fig. 3.13). This can be seen in Figure 3.9_c where the intensity of the OH stretching band decreases and shifts to a lower wavenumber of 3595 cm^{-1} forming a symmetric peak that can be identified as the protons located in the 8-MR.

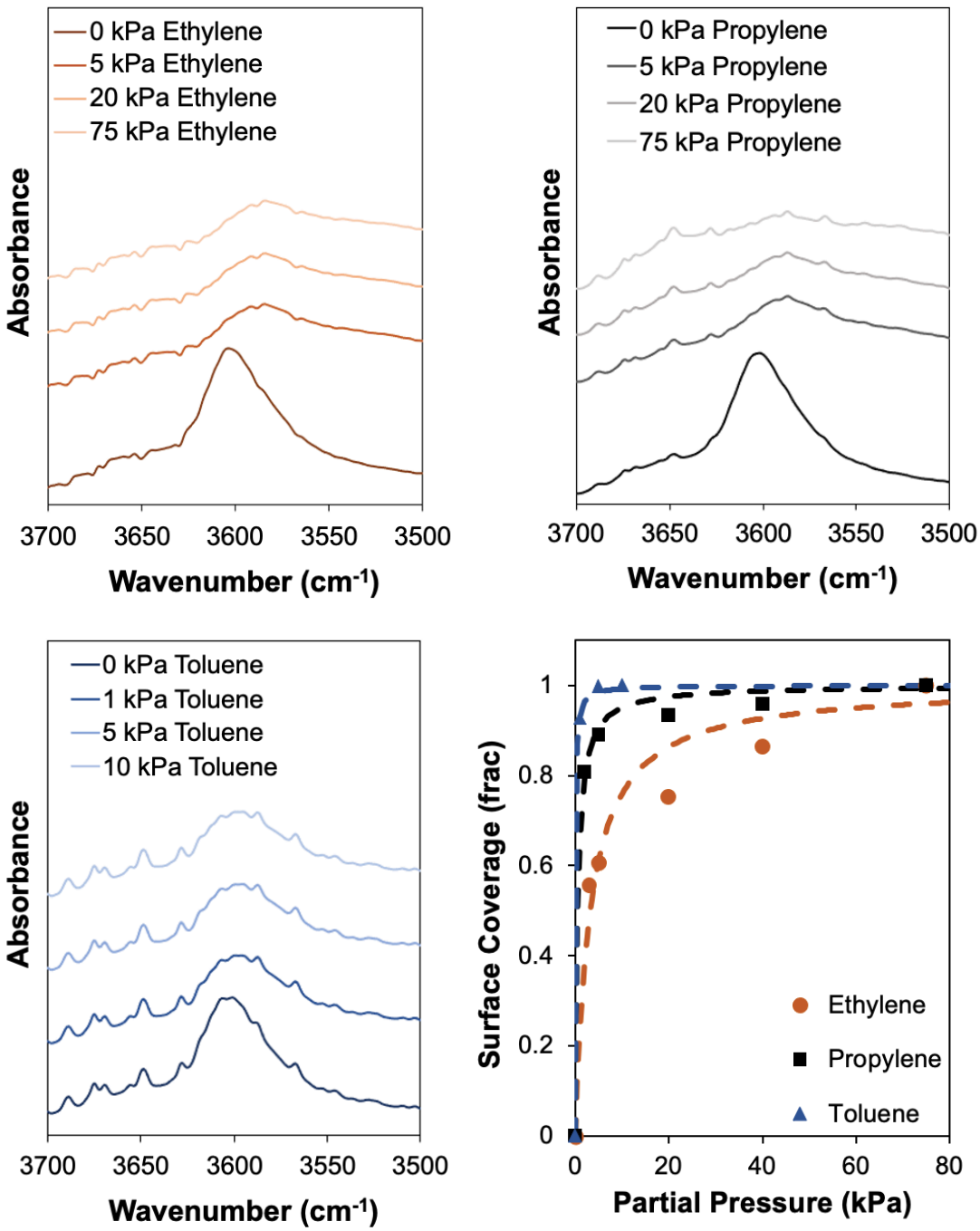

Figure 3.9 Infrared spectra of H^+-MOR (OH region) in contact with (a) ethylene (0-75 kPa), (b) propylene (0-75 kPa), (c) toluene (0-10 kPa), and (d) Surface coverages based on OH region as a function of ethylene, propylene, and toluene pressures (473K).

Fractional surface coverage of each species can be derived from the OH band intensity at different partial pressures. Figure 3.9_d shows the fractional surface coverage of ethylene, propylene, and toluene as a function of partial pressure on unexchanged H^+-MOR. Fractional surface coverage follows Langmuiran adsorption behavior due to the isolated nature of zeolite protons expressed by Eqn 3.1.[38] The equilibrium constant (K_{eq}) for ethoxide, isopropoxide, and toluene, calculated using infrared spectroscopy, are located in Table 1. In the case of ethylene, surface saturation was reached above 40 kPa while propylene reached full surface coverage at 20 kPa. Toluene reached surface saturation at partial pressures lower than both alkenes (< 10 kPa). These equilibrium constant results are comparable to Sarazen et al who measured equilibrium constants on TON and calculated a K_{eq} of 0.07 ± 0.006 and 0.35 ± 0.19 for ethoxide and isopropoxide formation respectively.[38]

Table 3.1 Measured equilibrium constants (K_{eq}) on H^+-MOR for C_2-C_3 alkoxides formations from ethylene and propylene and π-Toluene from in-situ infrared spectra (Fig. 3.9_d; 473 K)

Species	K_{eq} (kPa^{-1})	ΔG_{503K} (kJ/mol)
Ethoxide	0.3 ± 0.1	5
Isopropoxide	1.9 ± 0.2	-3
π-Toluene	13 ± 2	-10

The larger K_{eq} for toluene compared to those for ethoxide and propoxide suggest that the H^+ sites located within the 12-MR are covered with π-bonded toluene which can react with ethylene to form ethyltoluene. Conclusions from infrared spectroscopy are consistent with kinetic behavior (Fig. 3.5), which shows that the reaction linearly depends on ethylene and does not depend on toluene. Toluene alkylation thus would follow the concerted pathway where

ethylene would react with π-bonded toluene instead of forming an ethoxide. This reaction mechanism has been suggested in literature by Hansen et al.[29] Molecule orientation using DFT also showed that alkenes and their alkoxides preferentially utilize space offered by the side channel that connects the 8 MR and 12 MR (Fig. 3.10). Due to the size of the side channel, π-bonded toluene and benzene are restricted to adsorb completely in the 8-MR channel (Fig. 3.10). Adsorbates in the larger 12-MR are less constrained do not utilize the side channel (Fig. 3.11).

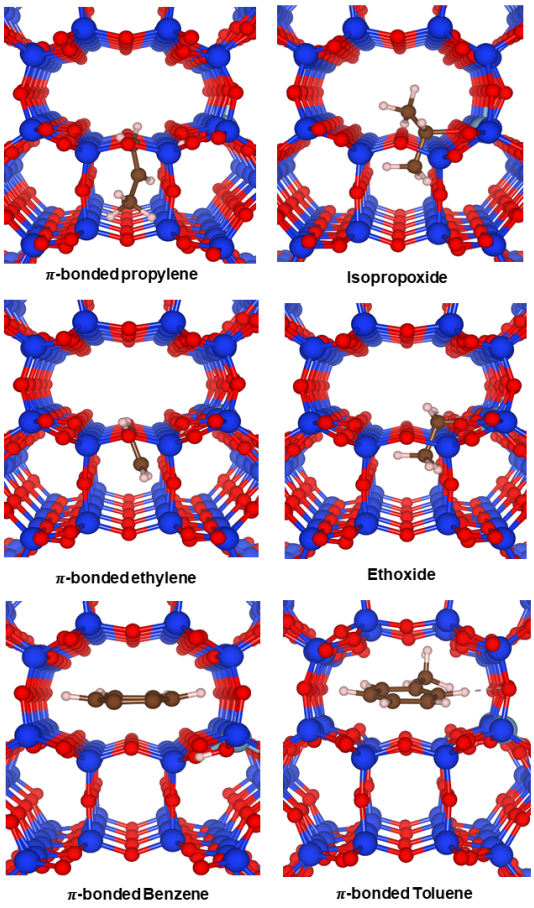

Figure 3.10 DFT-derived geometries of bound species on the H^+ sites located within 8 MR in MOR zeolite (Al-T1).

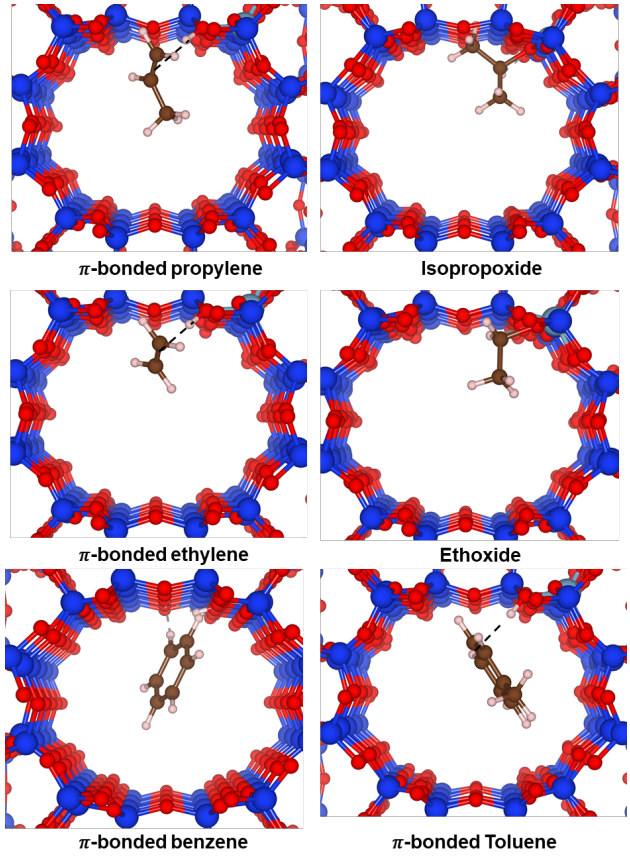

Figure 3.11 DFT-derived geometries of bound species on the H^+ sites located within 12 MR in MOR zeolite (Al-T2).

Van der Waals (vdW) interactions are well-known to critically contribute to the adsorption of aromatic hydrocarbons in zeolites.[10,38,39] Therefore, the quantum-mechanical (QM) and vdW components of adsorption energies were separated from the total adsorption energy, as described by Eqn 3.3, for ethoxide, isopropoxide, benzene, and toluene (Fig. 3.12). In the 8-MR, the magnitude of these components correlates strongly with the size of the adsorbate (Fig.3.12_b). The QM and total electronic adsorption energies become more positive with the adsorbate's size and a corresponding increase in magnitude of the vdW component. This trend is consistent with previous DFT-D3 calculations of alkenes and their alkoxides in the 10-MR channels of TON zeolite, which was determined to be comparable with MOR.[38] The trend is less

distinct in the 12-MR channel, where adsorbates are less confined and vdW contributions are smaller than in the 8-MR. The vdW components of adsorption in the 8-MR (12-MR) channel range from -292 kJ/mol (-136 kJ/mol) for toluene to -80 kJ/mol (-47 kJ/mol) for ethoxide.

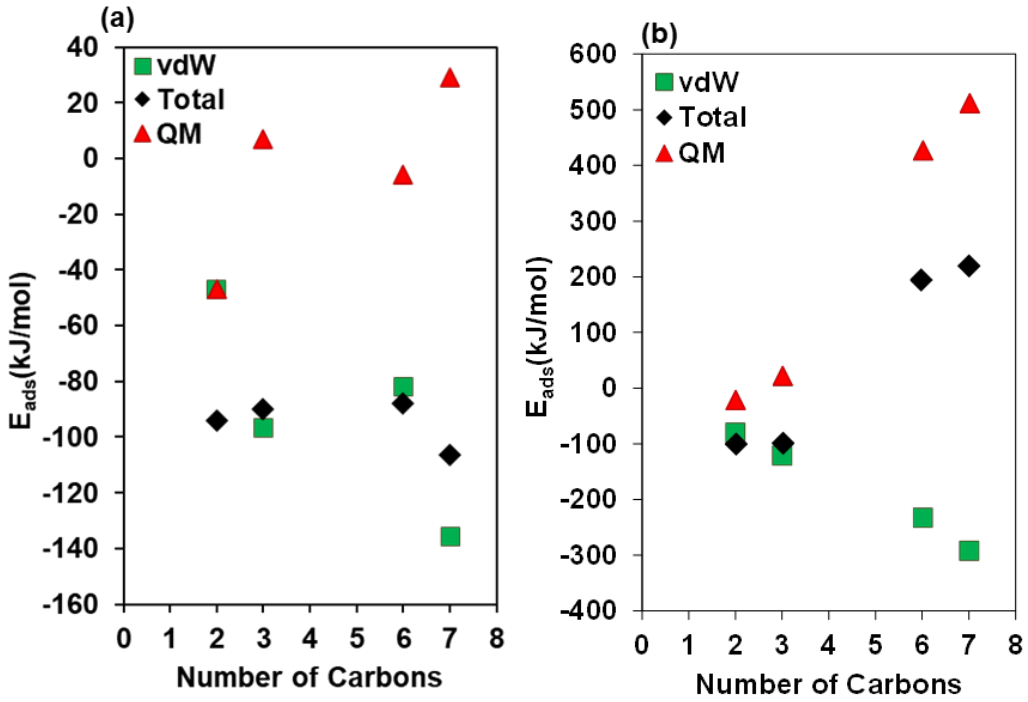

Figure 3.12 DFT-derived electronic energies for formation of p-Ethoxide, p-Propoxide, π-Toluene from respective gaseous molecules on the acidic H+ sites located in (a) 12 MR (Al-T2) and (b) 8 MR (Al-T1) on MOR. Calculated total electronic energies (◆) are broken down into two components: the quantum mechanical (▲) and the van der Waals (■).

In both the 8-MR and 12-MR channels, alkoxides are more stable than their π - alkenes, in agreement with previous DFT studies of alkylation alkene and alkoxide stabilities in 10-MR TON.[38] The magnitudes of adsorption energies are comparable with calculated enthalpies of adsorption in 10-MR TON for ethene (-63 kJ/mol), ethoxide (-93 kJ/mol), propene (-82 kJ/mol), and isopropoxide (-105 kJ/mol).[38] This also agrees with the spectroscopic evidence of alkoxide formation upon the introduction of alkenes to H^+-MOR. Furthermore, the formation of both π - alkenes and alkoxides is more favorable in the 8-MR than in the 12-MR, facilitated by significant

vdW interactions (Fig. 3.12, trend of QM/Total/vdW). Although van der Waals interactions allow some compensation for forcing large adsorbates (benzene, toluene) into the confinement of the 8-MR channel, they cannot dominate the repulsive interactions of these adsorbates with the framework. The total adsorption energies of benzene and toluene (Fig. 3.13) in the 8-MR are thermodynamically unfavorable ($E_{ads} > 0$), exceeding 190 kJ/mol; it is therefore improbable that these hydrocarbons will adsorb in 8-MR, in agreement with spectroscopic observations in section 3.4.2. In contrast, the adsorption of benzene and ethylene is thermodynamically favorable (E_{ads} = -88 kJ/mol and -64 kJ/mol, respectively) in the 12-MR with magnitudes comparable with a DFT-D3 study of benzene alkylation in the 12-MR of H^+-MOR, which predicted benzene and ethylene adsorption energies of -100 kJ/mol and -60 kJ/mol, respectively.[10]

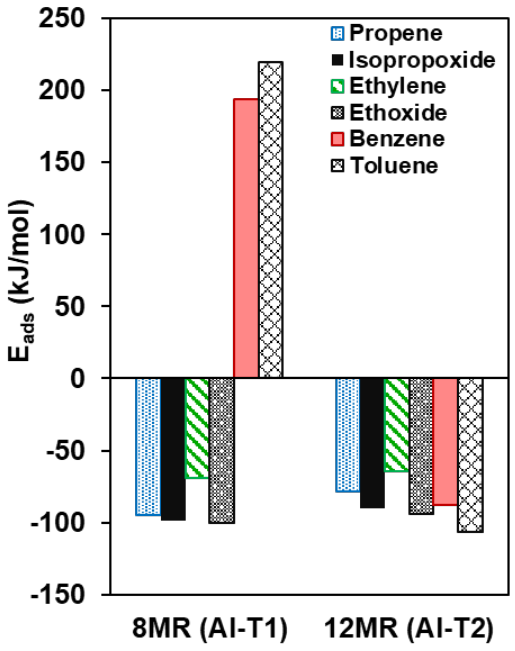

Figure 3.13 DFT-derived adsorption energies of bound species located on the H^+ sites located within 8 MR (Al-T1) and 12 MR (Al-T2) in MOR zeolite.

The most strongly-bound adsorbate is toluene adsorbed at Al-T2 in the 12-MR (E_{ads} = -107 kJ/mol), with a magnitude in agreement with previous DFT studies with vdW corrections.[11] This is followed by ethoxide and isopropoxide (E_{ads} = -94 kJ/mol and -90 kJ/mol, respectively). This trend in stability (toluene > alkoxide intermediate) is consistent with the spectroscopically observed fractional surface coverages and derived equilibrium constants that predict toluene will rapidly saturate the active sites in H^+-MOR, followed by isopropoxide and ethoxide (Fig.3.9_d, Table 3.1).

3.5 Conclusion

In this work, the role of micropores on the reactivity, selectivity, and stability of toluene alkylation on MOR were studied. Selective titration of H^+ sites out of the 8-MR significantly improved catalyst stability with a 6-fold decrease in deactivation compared to unexchanged H^+-MOR. Improved stability was attributed to the reduction in alkene dimerization which was found to preferentially occur within the 8-MR. Toluene alkylation reaction pathways were probed using kinetic, spectroscopic, and theoretical techniques which showed that the H+ sites are saturated with π-bonded toluene, which reacts with ethylene to form ethyl toluene products. These results can be utilized to aid in catalyst design strategies to improve catalytic performance by providing insight into how the microporous structure can be tuned to fit the transition state of the desired product leading to improved selectivity.

3.6 Acknowledgements

This work is supported by the startup funding from Colorado School of Mines and by ACS-PRF. This work used the Extreme Science and Engineering Discovery Environment (XSEDE), which is supported by National Science Foundation grant number ACI-1548562[40],

utilizing Stampede2 at the Texas Advanced Computing Center through allocation TG-CHM210005. This research also used resources of the National Energy Research Scientific Computing Center (NERSC), a U.S. Department of Energy Office of Science User Facility located at Lawrence Berkeley National Laboratory, operated under Contract No. DE-AC02-05CH11231 using NERSC award BES-ERCAP0021167.

CHAPTER 4

CONCLUSIONS AND FUTURE WORK

4.1 Conclusions

Zeolite such as MOR, MWW, and MFI have been used commercially for alkylation processes; however, they often suffer from catalyst deactivation. High benzene to alkene ratio is utilized to combat catalyst deactivation but often result in additional process units to recovery benzene and to convert transalkylated products to desired monoalkylated products. In this work, we control the distribution of protons within MOR to examine the impact the microporous structure of MOR has on the reactivity, selectivity, and stability of toluene alkylation. Here we focus on toluene alkylation to avoid the use of highly toxic benzene while still exhibiting similar reaction scheme as benzene alkylation. To conduct this experimental work, a reactor system was engineered to withstand the high pressure and temperature requirements associated with benzene alkylation.

Here we selectively titrated all H^+ site from the 8-MR to assess the role of the 8-MR in mediating desired product formation. Selective titration of H^+ sites out of the 8-MR significantly improved catalyst stability with a deactivation constant of 0.02 ks^{-1} which is 6-fold lower than unexchanged H^+- MOR. Improved stability was attributed to the reduction in alkene dimerization which was found to preferentially occur within the 8-MR.

Toluene alkylation reaction pathways were probed using kinetic, spectroscopic, and theoretical methods to determine the mechanism involved in reactant binding. Kinetic measurements showed that the reaction rate order to be zero in toluene and first in ethylene meaning that toluene pressure changes did not impact the rate suggestive of the concerted pathway. Derivation of rate equations for the stepwise and concerted pathway resulted in indistinguishable rates therefore spectroscopic and theoretical methods were employed to determine the surface binding of reactants. Infrared spectra showed coverage of alkoxide species for both ethylene and propylene on the proton site of MOR. Upon the introduction of toluene, the H+ sites were saturated with π-bonded toluene, which reacts with ethylene to form ethyl toluene products. The resulting infrared measurements led to equilibrium constants, K_{eq}, where toluene > propylene > ethylene. These results were confirmed through DFT calculations which showed the same trend in equilibrium constants thus predicting that toluene will rapidly saturate the active sites in H^+-MOR, followed by ethoxide and isopropoxide. These results can be utilized to improve catalyst synthesis for benzene alkylation by providing insight into how the microporous structure can be tuned to fit the transition state of the desired product leading to improved selectivity.

4.2 Future Work

Further research will be performed on MOR as well as other zeolites. For MOR, we plan to continue experimentation with ethylene on sodium exchanged samples with varying amounts of sodium. Reactions at different temperatures between 473-523 K will also be performed to determine temperature dependence and calculate apparent activation energy, Ea. In addition to ethylene, we plan to perform experiments using propylene as our alkene of choice. Based on our

DFT results, propylene has a larger K_{eq} and molecule size than ethylene so we would like to look at reactivity and selectivity for toluene alkylation with propylene.

To normalize rates among samples, several techniques will be utilized to determine the number of protons in the unexchanged and sodium exchanged samples. Temperature programmed desorption (TPD) is a frequently employed technique to characterize zeolite acidity by determining the number of acidic sites, or protons in the sample. This technique will be employed on both unexchanged and sodium exchanged samples to calculate extent of sodium exchange. Ammonia capped unexchanged samples will be heated to 500°C at 10°C/min under helium while utilizing mass spectrometry (MS) to determine the amount of desorbed ammonia. For exchanged samples, ammonia will be introduced to the sample at 100°C then subsequently heated to following the same protocol of 500°C at 10°C/min under helium to determine amount of ammonia desorbed. TPD will allow us to compare zeolite reactivity based on number of active sites resulting in accurate rate normalization across zeolite samples. In addition, we plan to use inductively coupled plasma optical emission spectroscopy (ICP-OES) to determine amount of Na present in exchanged samples.

In addition to MOR, several other zeolites (MFI, BEA, and MWW) have been suggested to work for benzene alkylation. Future work will include analysis of a range of zeolites with diverse pore structures to determine the impact that that pore size has on catalytic performance. In this way, we hope to find the optimum pore size for monoalkylated product formation. Mesoporous samples will also be tested to understand the acidity and selectivity of protons without confinement affects. Zeolites will be tested and measured against each other in terms of stability and selectivity for benzene alkylation. Based on DFT calculations, Acharya et al recommends MFI as a possible candidate for benzene alkylation due to its channel's ability to confine the

reactant species without obvious repulsion based on DFT and MD modeling so we may begin with this zeolite.[28]

Future work will also extend to DFT calculations and include conducting transition-states searches to investigate the effects of confinement upon rates of ethylene dimerization and the alkylation of aromatic hydrocarbons (e.g., benzene, toluene). Vibrational frequency analyses will be completed to calculated temperature-corrected energetics, including adsorption energies and activation barriers.

REFERENCES

1. Palčić, A. & Valtchev, V. Analysis and control of acid sites in zeolites. *Applied Catalysis A: General* vol. 606 (2020).

2. Li, Y., Li, L. & Yu, J. Applications of Zeolites in Sustainable Chemistry. *Chem* vol. 3 928–949 (2017).

3. Siffert, S., Gaillard, L. & Su, B.-L. *Alkylation of benzene by propene on a series of Beta zeolites: toward a better understanding of the mechanisms*. *Journal of Molecular Catalysis A:Chemical* vol. 153 www.elsevier.comrlocatermolcata (2000).

4. Degnan, T. F., Smith, C. M. & Venkat, C. R. *Alkylation of aromatics with ethylene and propylene: recent developments in commercial processes*. *Applied Catalysis A: General* vol. 221 (2001).

5. Rastegar, S. F. *et al.* Analysis of decisive structural parameters of zeolites for alkylation of benzene with ethylene. *Applied Catalysis A: General* **591**, (2020).

6. Atanda, L. A., Aitani, A. M. & Al-Khattaf, S. S. Experimental and kinetic studies of ethyltoluenes production via different alkylation reactions. *Chemical Engineering Research and Design* **95**, 34–46 (2015).

7. Emana, A. N. & Chand, S. Alkylation of benzene with ethanol over modified HZSM-5 zeolite catalysts. *Applied Petrochemical Research* **5**, 121–134 (2015).

8. Derouane, E. G. *Zeolites as solid solvents 1*. *Journal of Molecular Catalysis A: Chemical* vol. 134 (1998).

9. Khan, W., Jia, X., Wu, Z., Choi, J. & Yip, A. C. K. Incorporating hierarchy into conventional zeolites for catalytic biomass conversions: A review. *Catalysts* vol. 9 (2019).

10. Xing, S. Y., Liu, K. K., Wang, T. F. & Han, M. H. First principles study on the alkylation of benzene with ethene over different zeolites: Insight into the intrinsic mechanism and structure-reactivity relationship. *Molecular Catalysis* **512**, (2021).

11. Rozanska, X., Barbosa, L. A. M. M. & van Santen, R. A. A periodic density functional theory study of cumene formation catalyzed by H-mordenite. *Journal of Physical Chemistry B* **109**, 2203–2211 (2005).

12. Chai, Y., Dai, W., Wu, G., Guan, N. & Li, L. Confinement in a Zeolite and Zeolite Catalysis. *Accounts of Chemical Research* **54**, 2894–2904 (2021).

13. Sastre, G. & Corma, A. The confinement effect in zeolites. *Journal of Molecular Catalysis A: Chemical* **305**, 3–7 (2009).

14. Gounder, R. & Iglesia, E. The catalytic diversity of zeolites: Confinement and solvation effects within voids of molecular dimensions. *Chemical Communications* **49**, 3491–3509 (2013).

15. Csicsery, S. M. *Shape-selective catalysis inzeolites*.

16. Cherkasov, N., Vazhnova, T. & Lukyanov, D. B. Quantitative infra-red studies of Brønsted acid sites in zeolites: Case study of the zeolite mordenite. *Vib Spectrosc* **83**, 170 179 (2016).

17. Lei, Z., Liu, L. & Dai, C. Insight into the reaction mechanism and charge transfer analysis for the alkylation of benzene with propylene over H-beta zeolite. *Molecular Catalysis* **454**, 1–11 (2018).

18. Al-Kinany, M. C. *et al.* Selective zeolite catalyst for alkylation of benzene with ethylene to produce ethylbenzene. *Applied Petrochemical Research* **2**, 73–83 (2012).

19. Han, M., Lin, S. & Roduner, E. *Study on the alkylation of benzene with propylene over H zeolite*. *Applied Catalysis A: General* vol. 243 (2003).

20. Cheng, Z. *et al.* Role of bronsted acid sites within 8-MR of mordenite in the deactivation roadmap for dimethyl ether carbonylation. *ACS Catalysis* **11**, 5647–5657 (2021).

21. Bhan, A., Allian, A. D., Sunley, G. J., Law, D. J. & Iglesia, E. Specificity of sites within eight-membered ring zeolite channels for carbonylation of methyls to acetyls. *J Am Chem Soc* **129**, (2007).

22. Gounder, R. & Iglesia, E. Catalytic consequences of spatial constraints and acid site location for monomolecular alkane activation on zeolites. *J Am Chem Soc* **131**, 1958–1971 (2009).

23. Sarazen, M. L., Doskocil, E. & Iglesia, E. Catalysis on solid acids: Mechanism and catalyst descriptors in oligomerization reactions of light alkenes. *Journal of Catalysis* **344**, 553–569 (2016).

24. Du, Y., Wang, H. & Chen, S. *Study on alkylation of benzene with ethylene over-zeolite catalyst to ethylbenzene by in situ IR*. *Journal of Molecular Catalysis A: Chemical* vol. 179 (2002).

25. Corma, A., Martínez-Soria, V. & Schnoeveld, E. Alkylation of benzene with short-chain olefins over MCM-22 zeolite: Catalytic behaviour and kinetic mechanism. *Journal of Catalysis* **192**, 163–173 (2000).

26. Xing, S., Liu, K., Wang, T., Zhang, R. & Han, M. Elucidation of the mechanism and structure-reactivity relationship in zeolite catalyzed alkylation of benzene with propylene. *Catalysis Science and Technology* **11**, 2792–2804 (2021).

27. Wang, D. *et al.* Recent Advances for Selective Catalysis in Benzene Methylation: Reactions, Shape-Selectivity and Perspectives. *Catalysis Surveys from Asia* vol. 25 347 361 (2021).

28. Acharya, D. *et al.* Stepwise or Concerted Mechanisms of Benzene Ethylation Catalyzed by Zeolites? Theoretical Analysis of Reaction Pathways. *Catalysis Letters* **151**, 3048 3056 (2021).

29. Hansen, N. & Keil, F. J. Multiscale modeling of reaction and diffusion in zeolites: From the molecular level to the reactor. *Soft Materials* **10**, 179–201 (2012).

30. Perego, C. & Ingallina, P. *Recent advances in the industrial alkylation of aromatics: new catalysts and new processes*. *Catalysis Today* vol. 73 (2002).

31. Laredo, G. C., Castillo, J. J., Navarrete-Bolaños, J., Perez-Romo, P. & Lagos, F. A. Benzene reduction in gasoline by alkylation with olefins: Comparison of Beta and MCM 22 catalysts. *Applied Catalysis A: General* **413–414**, 140–148 (2012).

32. Odedairo, T. & Al-Khattaf, S. Comparative study of zeolite catalyzed alkylation of benzene with alcohols of different chain length: H-ZSM-5 versus mordenite. *Catalysis Today* **204**, 73–84 (2013).

33. Kresse, G. & Furthmiiller B ', J. *Efficiency of ab-initio total energy calculations for metals and semiconductors using a plane-wave basis set*. *Computational Materials Science* vol. 6 (1996).

34. Kresse, G. & Furthmüller, J. Efficient iterative schemes for ab initio total-energy calculations using a plane-wave basis set. *Physical Review B* **54**, 11169–11186 (1996).

35. Hammer, B., Hansen, L. B. & Nørskov, J. K. Improved adsorption energetics within density-functional theory using revised Perdew-Burke-Ernzerhof functionals. *Phys. Rev. B* **59**, (1999).

36. Grimme, S., Ehrlich, S. & Goerigk, L. Effect of the damping function in dispersion corrected density functional theory. *J Comput Chem* **32**, 1456–1465 (2011).

37. Demuth, T., Benco, L., Hafner, J., Toulhoat, H. & Hutschka, F. Ab initio investigation of the adsorption of benzene in mordenite. *Journal of Chemical Physics* **114**, 3703–3712 (2001).

38. Sarazen, M. L. & Iglesia, E. Stability of bound species during alkene reactions on solid acids. *Proc Natl Acad Sci U S A* **114**, E3900–E3908 (2017).

39. Sarazen, M. L. & Iglesia, E. Effects of Charge, Size, and Shape of Transition States, Bound Intermediates, and Confining Voids in Reactions of Alkenes on Solid Acids. *ChemCatChem* **10**, 4028–4037 (2018).

40. Towns, J. *et al.* XSEDE: Accelerating Scientific Discovery. 62–74 (2014) doi:10.1109/MCSE.2014.80.

APPENDIX A

SUPPORTING INFORMATION

$$rate_{concerted} = k_2[C_2H_4 - H^*][C_7H_8]$$

$$Site\ balance \quad [\mathrm{L}] = [H^*] + [C_2H_4 - H^*] + [C_9H_{12} - H^*]$$

$$[C_2H_4 - H^*] = K_1[C_2H_4][H^*]$$

$$[C_9H_{12} - H^*] = K_3[C_9H_{12}][H^*]$$

$$\frac{[H^*]}{[\mathrm{L}]} = \frac{1}{1 + K_1[C_2H_4] + K_3[C_9H_{12}]}$$

$$rate_{concerted} = \frac{k_2K_1[C_2H_4][C_7H_8]}{1 + K_1[C_2H_4] + K_3[C_9H_{12}]}$$

Figure A.1 Derivation of rate equation for concerted pathway with π-bonded toluene.

APPENDIX B

COPYRIGHT APPROVAL

Approval for Figure 1.1

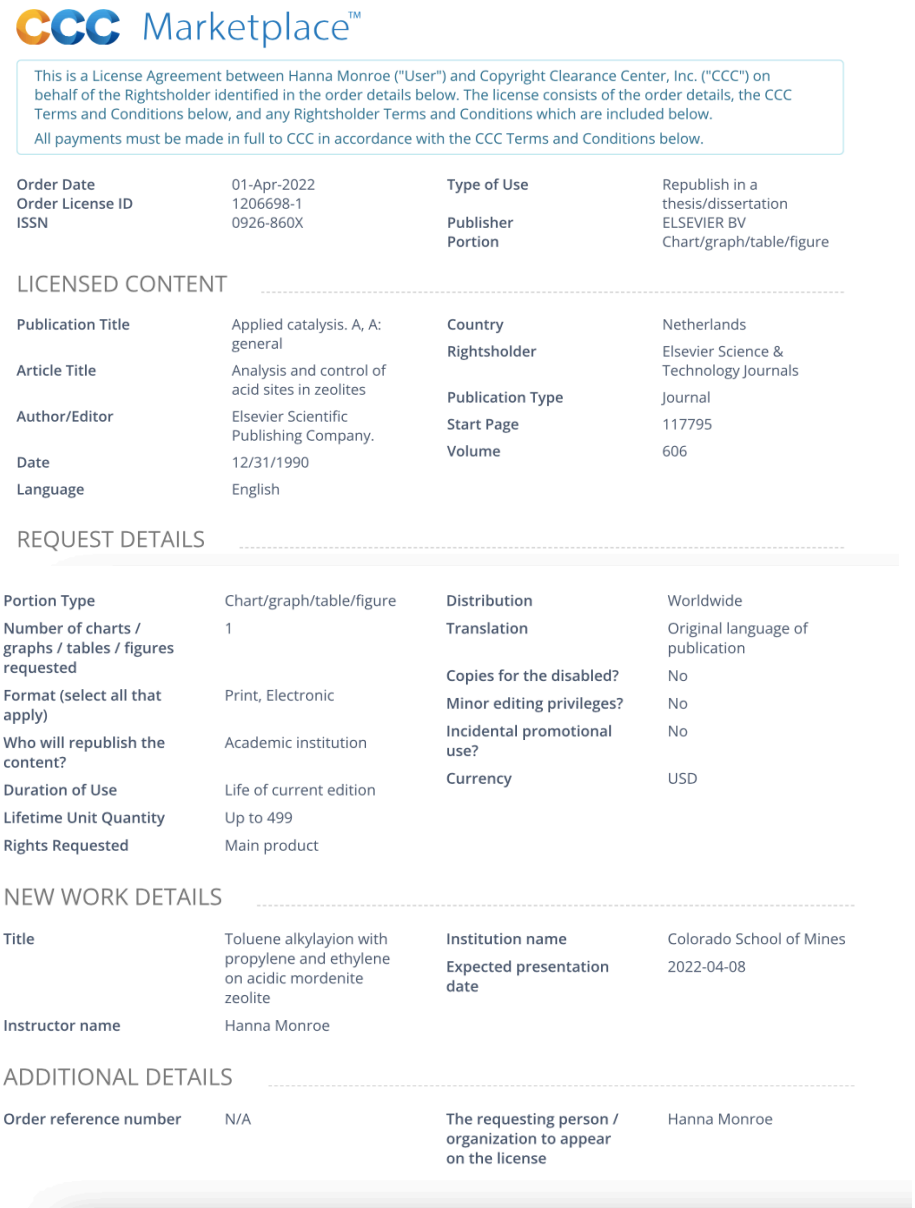

CCC Marketplace™

This is a License Agreement between Hanna Monroe ("User") and Copyright Clearance Center, Inc. ("CCC") on behalf of the Rightsholder identified in the order details below. The license consists of the order details, the CCC Terms and Conditions below, and any Rightsholder Terms and Conditions which are included below.

All payments must be made in full to CCC in accordance with the CCC Terms and Conditions below.

Order Date	01-Apr-2022	Type of Use	Republish in a thesis/dissertation
Order License ID	1206698-1		
ISSN	0926-860X	Publisher	ELSEVIER BV
		Portion	Chart/graph/table/figure

LICENSED CONTENT

Publication Title	Applied catalysis. A, A: general	Country	Netherlands
Article Title	Analysis and control of acid sites in zeolites	Rightsholder	Elsevier Science & Technology Journals
Author/Editor	Elsevier Scientific Publishing Company.	Publication Type	Journal
		Start Page	117795
Date	12/31/1990	Volume	606
Language	English		

REQUEST DETAILS

Portion Type	Chart/graph/table/figure	Distribution	Worldwide
Number of charts / graphs / tables / figures requested	1	Translation	Original language of publication
		Copies for the disabled?	No
Format (select all that apply)	Print, Electronic	Minor editing privileges?	No
Who will republish the content?	Academic institution	Incidental promotional use?	No
Duration of Use	Life of current edition	Currency	USD
Lifetime Unit Quantity	Up to 499		
Rights Requested	Main product		

NEW WORK DETAILS

Title	Toluene alkylayion with propylene and ethylene on acidic mordenite zeolite	Institution name	Colorado School of Mines
		Expected presentation date	2022-04-08
Instructor name	Hanna Monroe		

ADDITIONAL DETAILS

Order reference number	N/A	The requesting person / organization to appear on the license	Hanna Monroe

REUSE CONTENT DETAILS

Title, description or numeric reference of the portion(s)	Schematic representation of zeolite structure formation	**Title of the article/chapter the portion is from**	Analysis and control of acid sites in zeolites
Editor of portion(s)	Valtchev, Valentin; Palčić, Ana	**Author of portion(s)**	Valtchev, Valentin; Palčić, Ana
Volume of serial or monograph	606	**Issue, if republishing an article from a serial**	N/A
Page or page range of portion	117795	**Publication date of portion**	2020-09-24

RIGHTSHOLDER TERMS AND CONDITIONS

Elsevier publishes Open Access articles in both its Open Access journals and via its Open Access articles option in subscription journals, for which an author selects a user license permitting certain types of reuse without permission. Before proceeding please check if the article is Open Access on http://www.sciencedirect.com and refer to the user license for the individual article. Any reuse not included in the user license terms will require permission. You must always fully and appropriately credit the author and source. If any part of the material to be used (for example, figures) has appeared in the Elsevier publication for which you are seeking permission, with credit or acknowledgement to another source it is the responsibility of the user to ensure their reuse complies with the terms and conditions determined by the rights holder. Please contact permissions@elsevier.com with any queries.

CCC Terms and Conditions

1. Description of Service; Defined Terms. This Republication License enables the User to obtain licenses for republication of one or more copyrighted works as described in detail on the relevant Order Confirmation (the "Work(s)"). Copyright Clearance Center, Inc. ("CCC") grants licenses through the Service on behalf of the rightsholder identified on the Order Confirmation (the "Rightsholder"). "Republication", as used herein, generally

2. The terms set forth in the relevant Order Confirmation, and any terms set by the Rightsholder with respect to a particular Work, govern the terms of use of Works in connection with the Service. By using the Service, the person transacting for a republication license on behalf of the User represents and warrants that he/she/it (a) has been duly authorized by the User to accept, and hereby does accept, all such terms and conditions on behalf of User, and (b) shall inform User of all such terms and conditions. In the event such person is a "freelancer" or other third party independent of User and CCC, such party shall be deemed jointly a "User" for purposes of these terms and conditions. In any event, User shall be deemed to have accepted and agreed to all such terms and conditions if User republishes the Work in any fashion.

3. Scope of License; Limitations and Obligations.

   3.1. All Works and all rights therein, including copyright rights, remain the sole and exclusive property of the Rightsholder. The license created by the exchange of an Order Confirmation (and/or any invoice) and payment by User of the full amount set forth on that document includes only those rights expressly set forth in the Order Confirmation and in these terms and conditions, and conveys no other rights in the Work(s) to User. All rights not expressly granted are hereby reserved.

   3.2. General Payment Terms: You may pay by credit card or through an account with us payable at the end of the month. If you and we agree that you may establish a standing account with CCC, then the following terms apply: Remit Payment to: Copyright Clearance Center, 29118 Network Place, Chicago, IL 60673-1291. Payments Due: Invoices are payable upon their delivery to you (or upon our notice to you that they are available to you for downloading). After 30 days, outstanding amounts will be subject to a service charge of 1-1/2% per month or, if less, the maximum rate allowed by applicable law. Unless otherwise specifically set forth in the Order Confirmation or in a separate written agreement signed by CCC, invoices are due and

Approval for Figure 1.2

CCC Marketplace™

This is a License Agreement between Hanna Monroe ("User") and Copyright Clearance Center, Inc. ("CCC") on behalf of the Rightsholder identified in the order details below. The license consists of the order details, the CCC Terms and Conditions below, and any Rightsholder Terms and Conditions which are included below.

All payments must be made in full to CCC in accordance with the CCC Terms and Conditions below.

Order Date	14-Mar-2022	**Type of Use**	Republish in a thesis/dissertation
Order License ID	1199630-1		
ISSN	2451-9294	**Publisher**	Elsevier Inc
		Portion	Image/photo/illustration

LICENSED CONTENT

Publication Title	Chem	**Publication Type**	e-Journal
Article Title	Applications of Zeolites in Sustainable Chemistry	**Start Page**	928
		End Page	949
Date	12/31/2015	**Issue**	6
Language	English	**Volume**	3
Country	United States of America		
Rightsholder	Elsevier Science & Technology Journals		

REQUEST DETAILS

Portion Type	Image/photo/illustration	**Distribution**	Worldwide
Number of images / photos / illustrations	1	**Translation**	Original language of publication
Format (select all that apply)	Print	**Copies for the disabled?**	No
		Minor editing privileges?	No
Who will republish the content?	Academic institution	**Incidental promotional use?**	No
Duration of Use	Life of current edition	**Currency**	USD
Lifetime Unit Quantity	Up to 499		
Rights Requested	Main product		

NEW WORK DETAILS

Title	Benzene Alkylation with ethylene and propylene on acidic mordenite zeolite	**Institution name**	Colorado School of Mines
		Expected presentation date	2022-04-08
Instructor name	Hanna Monroe		

ADDITIONAL DETAILS

Order reference number	N/A	**The requesting person / organization to appear on the license**	Hanna Monroe

REUSE CONTENT DETAILS

Title, description or numeric reference of the portion(s)	Figure 1. Selected Widely Used Zeolite Framework Types	**Title of the article/chapter the portion is from**	Applications of Zeolites in Sustainable Chemistry
Editor of portion(s)	Yu, Jihong; Li, Yi; Li, Lin	**Author of portion(s)**	Yu, Jihong; Li, Yi; Li, Lin
Volume of serial or monograph	3	**Issue, if republishing an article from a serial**	6
Page or page range of portion	928-949	**Publication date of portion**	2017-11-30

RIGHTSHOLDER TERMS AND CONDITIONS

Elsevier publishes Open Access articles in both its Open Access journals and via its Open Access articles option in subscription journals, for which an author selects a user license permitting certain types of reuse without permission. Before proceeding please check if the article is Open Access on http://www.sciencedirect.com and refer to the user license for the individual article. Any reuse not included in the user license terms will require permission. You must always fully and appropriately credit the author and source. If any part of the material to be used (for example, figures) has appeared in the Elsevier publication for which you are seeking permission, with credit or acknowledgement to another source it is the responsibility of the user to ensure their reuse complies with the terms and conditions determined by the rights holder. Please contact permissions@elsevier.com with any queries.

CCC Terms and Conditions

1. Description of Service; Defined Terms. This Republication License enables the User to obtain licenses for republication of one or more copyrighted works as described in detail on the relevant Order Confirmation (the "Work(s)"). Copyright Clearance Center, Inc. ("CCC") grants licenses through the Service on behalf of the rightsholder identified on the Order Confirmation (the "Rightsholder"). "Republication", as used herein, generally means the inclusion of a Work, in whole or in part, in a new work or works, also as described on the Order Confirmation. "User", as used herein, means the person or entity making such republication.

2. The terms set forth in the relevant Order Confirmation, and any terms set by the Rightsholder with respect to a particular Work, govern the terms of use of Works in connection with the Service. By using the Service, the person transacting for a republication license on behalf of the User represents and warrants that he/she/it (a) has been duly authorized by the User to accept, and hereby does accept, all such terms and conditions on behalf of User, and (b) shall inform User of all such terms and conditions. In the event such person is a "freelancer" or other third party independent of User and CCC, such party shall be deemed jointly a "User" for purposes of these terms and conditions. In any event, User shall be deemed to have accepted and agreed to all such terms and conditions if User republishes the Work in any fashion.

3. Scope of License; Limitations and Obligations.

    3.1. All Works and all rights therein, including copyright rights, remain the sole and exclusive property of the Rightsholder. The license created by the exchange of an Order Confirmation (and/or any invoice) and payment by User of the full amount set forth on that document includes only those rights expressly set forth in the Order Confirmation and in these terms and conditions, and conveys no other rights in the Work(s) to User. All rights not expressly granted are hereby reserved.

    3.2. General Payment Terms: You may pay by credit card or through an account with us payable at the end of the month. If you and we agree that you may establish a standing account with CCC, then the following terms apply: Remit Payment to: Copyright Clearance Center, 29118 Network Place, Chicago, IL 60673-1291. Payments Due: Invoices are payable upon their delivery to you (or upon our notice to you that they are available to you for downloading). After 30 days, outstanding amounts will be subject to a service charge of 1-1/2% per month or, if less, the maximum rate allowed by applicable law. Unless otherwise specifically set